C.P. No. 961

C.P. No. 961

MINISTRY OF TECHNOLOGY

AERONAUTICAL RESEARCH COUNCIL

CURRENT PAPERS

The Velocity Field near Non-lifting Delta Wings according to Supersonic Linearized Theory

by

R. S. Bartlett, M.A

LONDON: HER MAJESTY'S STATIONERY OFFICE

1967

PRICE 10s 6*d* NET

U.D.C. No. 533.693.3 : 531.112 : 533.6.011.5 : 517.945

C.P. No.961*
June 1966

THE VELOCITY FIELD NEAR NON-LIFTING DELTA WINGS ACCORDING TO SUPERSONIC LINEARIZED THEORY

by

R. S. Bartlett, M.A.

SUMMARY

The linearized theory of supersonic flow past thin wings is used to obtain expressions for the three components of velocity of the flow about a family of non-lifting, symmetrical delta wings having rhombic cross sections and subsonic leading edges. A Mercury Autocode programme has been written for their evaluation and results have been obtained for a particular wing for three Mach numbers and two values of the ratio of semi-span to centre-line chord. Curves of constant velocity, in planes normal to the free stream direction at and behind the trailing edge, are given for each velocity component.

---

* Replaces R.A.E. Technical Report No.66177 - A.R.C. 28453

CONTENTS

1 INTRODUCTION

This Paper is concerned with the calculation, according to linearized theory, of the velocity fields cf a family cf symmetrical delta wings at zero incidence in a supersonic stream. The cross-sections of the wings by planes normal to the stream are rhombic end their centre-sections are represented by polynomials of the fifth degree *containing four* arbitrary coefficients. The component of the free stream normal to the leading edge is subsonic. The three velocity components are expressed in closed form in terms of elementary functions. The evaluation of the velocity components has been programmed for automatic digital computation. As en example, the velocity components of the wing known as 'Lord V' (wing 5 of Ref.?) are calculated for several *values* of the similarity parameter βs, where $\beta^2 = M^2 - 1$ and s is the ratio cf the semispan to the length. The results are presented as contours or level curves of the components in three planes normal to the stream, at end-behind the trailing edge.

Wings of this type have formed the basis for a number cf studies (see, for example, Refs.2 and 3) aimed at the generation of volume distributions which combine low calculated wave-drag with pressure distributions which make it likely that the type of flow postulated in the theory will be realized. The main criterion for the realization of the flow, and so of the wave-drag as calculated by inviscid flow theory is the avoidance of pressure distributions on the wing-which are markedly unfavourable to the development of a boundary layer attached up to the trailing edge. However, it is not sufficient to consider conditions on the wing surface only. If the calculated pressure at the trailing edge of the wing is *well below free-stream pressure or* the angle between the upper and low surfaces of the wing at the trading edge is large, adjustment to free-stream conditions behind the wing through a simple trailing edge shock may not be possible. Instead thickening, or even separation, may extend over the rear part of the wing, as observed by Firmin[4]. As a first step in assessing the likelihood of this, a *means* of obtaining pressure distributions, according to linearized theory, in the plane of the wing behind the trailing edge was required. It was realized that if further progress was to be made, it would be necessary to investigate the development cf the trailing edge shock system in the real flow. The opportunity was therefore taken of including in the present computer programme the calculation for prints off the wing surface, in order to provide a starting point for such an investigation. 'Although it'was not possible to proceed with this investigation, some calculations of the flow field off the wing are presented for their intrinsic intcrest.

2 CALCULATION OF Tii VELOCITY COMPONENTS BY LINEARIZED THEORY

In order to calculate the velocity field around a wing in inviscid isentrcpic supersonic flow, it is necessary to simplify the partial differential

equation for the velocity potential. For thin wings, this simplification is achieved by linearization of the equation, which is allowable under the following conditions:

(i) the angle which any tangent plane to the wing surface makes with the undisturbed stream, and the rate of change of this angle along the wing, must both be small,

(ii) transonio and hypersonic flows must be excluded.

In the present note we confine our interest to symmetrical wings at zero incidence, for which, under the above restrictions (i) and (ii), the perturbation velocity potential can be expressed in terms of a certain double integral, whose value must, in general, be evaluated numerically, a process whioh is complicated by the singular behaviour of the integrand. For wings of simple geometry, however, at least one of the integrations may be performed analytically. In the present case, the same applies to the seoond integration (see Section 3).

Let x, y, z be a right-handed coordinate system with origin O at the apex of the wing, x-axis along the free-stream direction and e-axis normal to the plane of the wing and vertically upward. The perturbation velocity potential is then given, in linear theory, by the solution of the equation

$$\beta^2 \phi_{xx} - \phi_{yy} - \phi_{zz} = 0. \qquad (1)$$

which satisfies the following boundary conditions:

$$\left(\frac{\partial \phi}{\partial z}\right)_{z=0} = 0 \qquad \text{outside the wing} \qquad (2)$$

$$\left(\frac{\partial \phi}{\partial z}\right)_{z=0} = U \left(\frac{\partial z(x,y)}{\partial x}\right)_{z=z(x,y)} \quad \text{on the wing ,} \qquad (3)$$

and vanishes upstream of the wing.

Here $z = z(x,y)$ is the equation of the upper surface of the sing. To the accuracy of linear theory, it is sufficient to satisfy (3)in the plane of the wing, $z = 0$, rather than on the wing itself, Under these conditions, equation (I) has the (unique) solution

$$\phi(x,y,z) = -\frac{U}{\pi} \iint_{\tau} \frac{\partial z(x',y')}{\partial x'} \frac{dx'\,dy'}{\sqrt{(x-x')^2 - \beta^2 (y-y')^2 - \beta^2 z^2}} \qquad (4)$$

where the area of integration, τ, is that part of the wing which lies inside the forward Mach cone from the point (x,y,z). It is bounded by the two leading edges of the wing, by the hyperbola ABCD, in which the forward Mach cone intersects the wing plane, and, possibly, by part of the trailing edge of the wing if the apex, C, of the hyperbola lies downstream of it (see Fig.1). The curve ABCD is given by the equation

$$z' = 0 \ , \ (x-x')^2 - \beta^2 (y-y')^2 - \beta^2 z^2 = 0 \ ,$$

In view of the symmetry about the planes $y = 0$ and $z = 0$, it is sufficient to consider the quadrant for which y and z are positive or zero.

Consider any function $f(x',y')$ defined in the plane of the wing, and suppose $y \geq 0$ and $z \geq 0$. Then, since the leading edges are taken to be subsonic (see Fig.1),

$$\iint_{\tau} f(x',y')\,dx'\,dy' = \int_{x'=0}^{\tilde{x}_M} \int_{y'=\bar{y}}^{\bar{\bar{y}}} f(x',y')\,dx'\,dy' - \int_{x'=0}^{\tilde{x}_A} \int_{y'=\bar{y}}^{-sx'} f(x',y')\,dx'\,dy' - \int_{x'=0}^{\tilde{x}_D} \int_{y'=sx'}^{\bar{\bar{y}}} f(x',y')\,dx'\,dy' \qquad (5)$$

where $x_M = x_C$ if C is behind the leading edge, or x_D otherwise;

x_A, x_C and x_D are the x-coordinates of the points A, C and D (see Appendix A);

the symbol $\tilde{x}_M$ denotes $\min(1, x_M)$, and similarly for $\tilde{x}_A$, etc.;

$\bar{\bar{y}} = y + \frac{1}{\beta}\sqrt{(x-x')^2 - \beta^2 z^2}$;

$\bar{y} = y - \frac{1}{\beta}\sqrt{(x-x')^2 - \beta^2 z^2}$;

s is the semi-span of the wing, which is taken to be of unit length.

For wings of delta planform and rhombic cross-section, as considered here, $z(x',y')$ is given by

$$z(x',y') = z(x',0)\left(1 - \frac{|y'|}{sx'}\right) \tag{6}$$

where $z = z(x',0)$ is the shape of the centre-section.

It follows that

$$\frac{\partial z(x',y')}{\partial x'} = g(x') + \frac{|y'|}{s} h(x') \tag{7A}$$

where

$$\left.\begin{aligned} g(x') &= \frac{\partial z(x',0)}{\partial x'} \\ h(x') &= -\frac{\partial}{\partial x'}\left(\frac{z(x',0)}{x'}\right) \end{aligned}\right\} \tag{7B}$$

In order to deal with the term involving $|y'|$, it is convenient to split up the first integral in equation (5), rewriting this equation in the form:

$$\begin{aligned} \iint_{\tau} f(x',y')\,dx'\,dy' = &\int_{x'=0}^{\tilde{x}_B} dx' \left(\int_{y'=\bar{y}}^{0} f(x',y')\,dy' + \int_{y'=0}^{\bar{\bar{y}}} f(x',y')\,dy' \right) \\ &+ \int_{x'=\tilde{x}_B}^{\tilde{x}_M} dx' \int_{y'=\bar{y}}^{\bar{\bar{y}}} f(x',y')\,dy' = \int_{x'=0}^{\tilde{x}_A} dx' \int_{y'=\bar{y}}^{-sx'} f(x',y')\,dy' \\ &- \int_{x'=0}^{\tilde{x}_D} dx' \int_{y'=sx'}^{\bar{\bar{y}}} f(x',y')\,dy' \end{aligned} \tag{5A}$$

where x_B is the x-coordinate of the point B and its value is also given in Appendix A. We can now evaluate $\phi(x,y,z)$ from equation (4) by giving a particular value to the function $f(x',y')$ in equation (5A), namely,

$$f(x',y') = \frac{\partial z(x',y')}{\partial x'} \cdot \frac{1}{\sqrt{(x-x')^2 - \beta^2 (y-y')^2 - \beta^2 z^2}}$$

ad by allowing equation (7A) to define $\partial z(x',y')/\partial x'$ both on and off the wing.

Whatever the value of the function $z(x',0)$, the integrations with respect to y' may be performed analytically for the wings considered here:

$$\int_0^Y f(x',y')\,dy' \equiv \int_0^Y \frac{\partial z(x',y')}{\partial x'} \frac{dy'}{\sqrt{(x-x')^2 - \beta^2 (y-y')^2 - \beta^2 z^2}}$$

$$= \left[-\frac{h(x')}{\beta^2 s} \sqrt{(x-x')^2 - \beta^2 (y-y')^2 - \beta^2 z^2} - \frac{1}{\beta}\left(g(x') + \frac{y}{s} h(x')\right) \right.$$

$$\left. -\sin^{-1}\left(\frac{\beta(y-y')}{\sqrt{(x-x')^2 - \beta^2 z^2}}\right) \right]_0^Y, \quad \text{for } Y > 0 \qquad (8A)$$

$$= \left[+\frac{h(x')}{\beta^2 s} \sqrt{(x-x')^2 - \beta^2 (y-y')^2 - \beta^2 z^2} - \frac{1}{\beta}\left(g(x') - \frac{y}{s} h(x')\right) \right.$$

$$\left. \sin^{-1}\left(\frac{\beta(y-y')}{\sqrt{(x-x')^2 - \beta^2 z^2}}\right) \right]_0^Y, \quad \text{for } Y < 0 \quad . \qquad (8B)$$

We require the values of the functions in square brackets in equations (8) for seven values of Y, namely

$$Y = 0, \quad -sx', \quad \bar{y} \qquad \text{[in (8B)]}$$

$$Y = 0, \quad sx', \quad \tilde{\bar{y}}, \quad \bar{y} \qquad \text{[in (8A)]}$$

We denote these values by B_N, $N = 1(1)7$, and their values are given in Appendix B. By evaluating the integral in equation (4) in the form given in equation (5A), we obtain the following expression for $\phi(x,y,z)$:

$$-\frac{\pi}{U}\phi(x,y,z) = \int_0^{\tilde{x}_B} [(B_1 - B_3) + (B_6 - B_4)]\,dx' + \int_{\tilde{x}_B}^{x_M} (B_6 - B_7)\,dx'$$

$$- \int_0^{\tilde{x}_A} (B_2 - B_3)\,dx' - \int_0^{\tilde{x}_D} (B_6 - B_5)\,dx' \quad . \qquad (9)$$

Substituting the values of the functions B_N into this equation, we obtain

$$
\begin{aligned}
-\frac{\pi}{U}\phi(x,y,z) = {} & \int_0^{\tilde{x}_B} \left\{ \frac{2h(x')}{\beta^2 s} \sqrt{(x-x')^2 - \beta^2 y^2 - \beta^2 z^2} + \frac{\pi}{\beta} g(x') + \frac{2yh(x')}{\beta s} \right. \\
& \left. \sin^{-1}\left(\frac{\beta y}{\sqrt{(x-x')^2 - \beta^2 z^2}} \right) \right\} ax' + \int_{\tilde{x}_B}^{\tilde{x}_M} \left\{ \frac{\pi}{\beta} \left(g(x') + \frac{y}{s} h(x') \right) \right\} dx' \\
& - \int_0^{x_A} \left\{ \frac{h(x')}{\beta^2 s} \sqrt{(x-x')^2 - \beta^2 (y+sx')^2 - \beta^2 z^2} + \frac{1}{\beta} \left(g(x') - \frac{y}{s} h(x') \right) \right. \\
& \left. \left(\frac{\pi}{2} - \sin^{-1}\left(\frac{\beta(y+sx')}{\sqrt{(x-x')^2 - \beta^2 z^2}} \right) \right) \right\} dx' \\
& - \int_0^{\tilde{x}_D} \left\{ \frac{h(x')}{\beta^2 s} \sqrt{(x-x')^2 - \beta^2 (y-sx')^2 - \beta^2 z^2} + \frac{1}{\beta} \left(g(x') + \frac{y}{s} h(x') \right) \right. \\
& \left. \left(\frac{\pi}{2} + \sin^{-1}\left(\frac{\beta(y-sx')}{\sqrt{(x-x')^2 - \beta^2 z^2}} \right) \right) \right\} dx'
\end{aligned}
\qquad \ldots (10)
$$

By differentiating this expression with respect to x, y and z, we can obtain expressions for the three velocity components.

These are as follows:

$$\frac{\pi}{U}\frac{\partial\phi}{\partial x} = \int_0^{\tilde{x}_B} \frac{2h(x')}{\beta^2 s}\cdot\frac{(x-x')}{[(x-x')^2-\beta^2 z^2]}\cdot\sqrt{(x-x')^2-\beta^2 y^2-\beta^2 z^2}\,dx' + \frac{\pi}{\beta}\left(g(\tilde{x}_M)-\frac{y}{s}h(\tilde{x}_M)\right)\frac{\partial\tilde{x}_M}{\partial x}$$

$$-\int_0^{\tilde{x}_A}\left\{\frac{h(x')}{\beta^2 s}\frac{(x-x')}{\sqrt{(x-x')^2-\beta^2(y+sx')^2-\beta^2 z^2}}+\left(g(x')-\frac{y}{s}h(x')\right)\frac{(sx'+y)(x-x')}{\sqrt{(x-x')^2-\beta^2(y+sx')^2-\beta^2 z^2}[(x-x')^2-\beta^2 z^2]}\right\}dx'$$

$$-\int_0^{\tilde{x}_D}\left\{\frac{h(x')}{\beta^2 s}\frac{(x-x')}{\sqrt{(x-x')^2-\beta^2(y-sx')^2-\beta^2 z^2}}+\left(g(x')+\frac{y}{s}h(x')\right)\frac{(sx'-y)(x-x')}{\sqrt{(x-x')^2-\beta^2(y-sx')^2-\beta^2 z^2}[(x-x')^2-\beta^2 z^2]}\right\}dx'$$

$$-\frac{\lambda\pi}{\beta}\left(g(\tilde{x}_D)+\frac{y}{s}h(\tilde{x}_D)\right)\frac{\partial\tilde{x}_D}{\partial x} \qquad . \tag{11}$$

$$-\frac{\pi}{U}\frac{\partial\phi}{\partial y} = \int_0^{\tilde{x}_B}\frac{2h(x')}{\beta s}\sin^{-1}\left(\frac{\beta y}{\sqrt{(x-x')^2-\beta^2 z^2}}\right)dx' + \frac{\pi}{\beta}\left(g(\tilde{x}_M)+\frac{y}{s}h(\tilde{x}_M)\right)\frac{\partial\tilde{x}_M}{\partial y} + \int_{\tilde{x}_B}^{\tilde{x}_M}\left(\frac{\pi h(x')}{\beta s}\right)dx'$$

$$+\int_0^{\tilde{x}_A}\left\{\frac{g(x')+x'h(x')}{\sqrt{(x-x')^2-\beta^2(y+sx')^2-\beta^2 z^2}}+\frac{h(x')}{\beta s}\left(\frac{\pi}{2}-\sin^{-1}\left(\frac{\beta(y+sx')}{\sqrt{(x-x')^2-\beta^2 z^2}}\right)\right)\right\}dx'$$

$$-\int_0^{\tilde{x}_D}\left\{\frac{g(x')+x'h(x')}{\sqrt{(x-x')^2-\beta^2(y-sx')^2-\beta^2 z^2}}+\frac{h(x')}{\beta s}\left(\frac{\pi}{2}+\sin^{-1}\left(\frac{\beta(y-sx')}{\sqrt{(x-x')^2-\beta^2 z^2}}\right)\right)\right\}dx'$$

$$-\frac{\lambda\pi}{\beta}\left(g(\tilde{x}_D)+\frac{y}{s}h(\tilde{x}_D)\right)\frac{\partial\tilde{x}_D}{\partial y} \qquad . \tag{12}$$

$$-\frac{\pi}{U}\frac{\partial\phi}{\partial z} = -\int_0^{\tilde{x}_B}\left\{\frac{2zh(x')}{s}\,\frac{\sqrt{(x-x')^2-\beta^2y^2-\beta^2z^2}}{[(x-x')^2-\beta^2z^2]}\right\}dx' + \frac{\pi}{\beta}\left(g(\tilde{x}_M)+\frac{y}{s}h(\tilde{x}_M)\right)\frac{\partial\tilde{x}_M}{\partial z}$$

$$+\int_0^{\tilde{x}_A}\left\{\frac{zh(x')}{s\sqrt{(x-x')^2-\beta^2(y+sx')^2-\beta^2z^2}}+\frac{\beta^2z\left(g(x')-\frac{y}{s}h(x')\right)(sx'+y)}{[(x-x')^2-\beta^2z^2]\sqrt{(x-x')^2-\beta^2(y+sx')^2-\beta^2z^2}}\right\}dx'$$

$$+\int_0^{\tilde{x}_D}\left\{\frac{zh(x')}{s\sqrt{(x-x')^2-\beta^2(y-sx')^2-\beta^2z^2}}+\frac{\beta^2z\left(g(x')+\frac{y}{s}h(x')\right)(sx'-y)}{[(x-x')^2-\beta^2z^2]\sqrt{(x-x')^2-\beta^2(y-sx')^2-\beta^2z^2}}\right\}dx'$$

$$-\frac{\lambda\pi}{\beta}\left(g(\tilde{x}_D)+\frac{y}{s}h(\tilde{x}_D)\right)\frac{\partial\tilde{x}_D}{\partial z} \quad . \tag{13}$$

In the above expressions, λ is given by

$$\lambda = \begin{cases}0\\1\end{cases} \text{ for } y \begin{cases}<\\\geq\end{cases} sx_D \quad . \tag{14}$$

3 EVALUATION OF THE VELOCITY COMPONENTS

In order to calculate the velocity components in particular cases, the oentre line thickness distribution has to be specified. There is considerable interest (see, for example, Refs.l-8) in the family of wings for which $z(x,0)$ is given by the following quintio polynomial:

$$z(x,0) = \frac{x}{2s}(1-x)\sum_{N=1}^{4}(c_{N-1}\,x^{N-1}),$$

for whioh the integrals given in equations (10)-(13) can be evaluated analytically. Four simple members of this family are given by

$$z_N(x,0) = \frac{x^N}{2s}(1-x), \quad N = 1\ (1)4$$

for which

$$\left.\begin{aligned} g(x) \equiv g_N(x) &= \frac{1}{2s}\left[N\,x^{N-1} - (N+1)\,x^N\right] \\ h(x) \equiv h_N(x) &= \frac{1}{2s}\left[N\,x^{N-1} - (N-1)\,x^{N-2}\right] \end{aligned}\right\} \qquad (15)$$

If the velooity potentials corresponding to these wings are given by

$$\phi = \phi_N, \qquad N = 1(1)4,$$

then that of any other member of the family is given by

$$\phi = c_0\phi_1 + c_1\phi_2 + c_2\phi_3 + c_3\phi_4,$$

and similar relations hold for the velocity components. It is sufficient, therefore, to evaluate the integrals which appear in the expressions for $\frac{\partial\phi_N}{\partial x}$, $\frac{\partial\phi_N}{\partial y}$, $\frac{\partial\phi_N}{\partial z}$ $(N = 1,2,3,4)$ by substitution of $g(x') = g_N(x')$ end $h(x') = h_N(x')$ into equations (11), (12) and (13)respeotively. This prcoess is simple in principle but entails a great *deal* of complicated algebra, best dealt with by classifying the integrals which arise. These are listed and evaluated in Appendices C and D respectively. In terms of these functions tne expressions for $\frac{\partial\phi_N}{\partial x}$, $\frac{\partial\phi_N}{\partial y}$ and $\frac{\partial\phi_N}{\partial z}$ become

$$-\frac{\pi}{U}\frac{\partial \phi_N}{\partial x} = -\frac{1}{\beta^2 s^2}\left[-N G_{N-1} + (N-1)\, G_{N-2}\right] + \frac{\pi}{\beta}\left[g_N(\tilde{x}_M) + \frac{y}{s} h_N(\tilde{x}_M)\right]\frac{\partial \tilde{x}_M}{\partial x} - \frac{1}{2s}\Big[2Ny\, Z_{N-1} - y\, Z_{N-1} - 2Ny\, Z_N - y\, Z_N - N\frac{y^2}{s} Z_{N-1}$$
$$+ (N-1)\frac{y^2}{s} Z_{N-2} + Ns\, Z_N - (N+1)\, s\, Z_{N+1}\Big]$$
$$+ \frac{1}{2\beta^2 s^2}\left[(N-1)(x\, V_{N-2} - V_{N-1}) - N(x\, V_{N-1} - V_N)\right] - \frac{1}{2s}\Big[-2Ny\, W_{N-1} + y\, W_{N-1} + 2Ny\, W_N + y\, W_N - N\frac{y^2}{s} W_{N-1}$$
$$+ (N-1)\frac{y^2}{s} W_{N-2} + Ns\, W_N - (N+1)\, s\, W_{N+1}\Big]$$
$$- \frac{\lambda\pi}{\beta}\left[g_N(\tilde{x}_D) + \frac{y}{s} h_N(\tilde{x}_D)\right]\frac{\partial \tilde{x}_D}{\partial x} \quad . \tag{15}$$

$$-\frac{\pi}{U}\frac{\partial \phi_N}{\partial y} = \frac{\pi}{2\beta s^2}\left(\tilde{x}_M^N - \tilde{x}_M^{N-1}\right) + \frac{\pi}{\beta}\left[g_N(\tilde{x}_M) + \frac{y}{s} h_N(\tilde{x}_M)\right]\frac{\partial \tilde{x}_M}{\partial y} + \frac{1}{2s^2}\left[y Z_N - y Z_{N-1} + s\, Z_{N+1} - s\, Z_N\right]$$
$$+ \frac{1}{2s^2}\left[y W_N - y W_{N-1} - s W_{N+1} + s W_N\right] - \frac{y}{s^2}\left[H_{N+10} - H_{N+9}\right] - \frac{\lambda\pi}{\beta}\left[g_N(\tilde{x}_D) + \frac{y}{s} h_N(\tilde{x}_D)\right]\frac{\partial \tilde{x}_D}{\partial y}$$
$$- \frac{\lambda\pi}{2\beta s^2}\left(\tilde{x}_D^N - \tilde{x}_D^{N-1}\right) \quad . \tag{16}$$

$$-\frac{\pi}{U}\frac{\partial \phi_N}{\partial z} = -\frac{z}{s^2}\left[NG_{N+3} - (N-1)\,G_{N+2}\right] + \frac{\pi}{\beta}\left[g_N(\tilde{x}_M) + \frac{y}{s}\,h_N(\tilde{x}_M)\right]\frac{\partial \tilde{x}_M}{\partial z}$$

$$+\frac{z}{2s^2}\left[NV_{N-1} - (N-1)\,V_{N-2}\right] + \frac{z}{2s^2}\left[NU_{N-1} - (N-1)\,U_{N-2}\right]$$

$$+\frac{\beta^2 z}{2s}\Big[(2N-1)\,y\,Y_{N+159} - (2N+1)\,y\,Y_{N+160} - \frac{Ny^2}{s}\,Y_{N+159}$$

$$+ (N-1)\,\frac{y^2}{s}\,Y_{N+158} + N s\,Y_{N+160} - (N+1)\,s\,Y_{N+161}\Big]$$

$$+\frac{\beta^2 z}{2s}\Big[-(2N-1)\,Y\,Y_{N+59} + (2N+1)\,Y\,Y_{N+60} - \frac{Ny^2}{s}\,Y_{N+59}$$

$$+ (N-1)\,\frac{y^2}{s}\,Y_{N+58} + N s\,Y_{N+60} - (N+1)\,s\,Y_{N+61}\Big]$$

$$-\frac{\lambda\pi}{\beta}\left[g_N(\tilde{x}_D) + \frac{y}{s}\,h_N(\tilde{x}_D)\right]\frac{\partial \tilde{x}_D}{\partial z} \quad . \qquad (17)$$

4 RESULTS

4.1 Accuracy of the calculations

The results given by Eminton[6] provide a limited check on the analysis and computer programme; limited because her method was restricted to the calculation of the streamwise component of velocity and that only on the wing surface. However the cases presented in Tables 1 and 2 of Ref.6 have been recalculated and the results found to agree.

No other calculations exist, as far as is known, for checking the programme for $z \neq 0$. However, the results have been found to be self-consistent in that the values of the velocity components are continuous functions everywhere, except across the trailing edge Mach wave, and in particular at $z = 0$, and at points at which λ and the derivatives of $\tilde{x}_A$, etc.are discontinuous.

Across the trailing edge Mach wave, the size of the discontinuity is found to be oorraot. Continuity at $z = 0$ is significant because at certain stages in the computer programme, one of two alternative sets of instructions is followed, depending on whether z is zero or non-zero.

4.2 Behaviour at lending and trailing edge Mach waves

4.2.1 Bow Mach wave

One limitation of linear theory affects all the results; namely that it predicts a bow Mach wave rather than a shock wave attached to the wing apex. However, Schlieren photographs' of these flows indicate that the shock waves are in fact very weak. Shock wave angles, θ_s, at the station x ≃ 0.6, have been measured from these photographs, for several wings of Lord V area distribution. These show that the ratio θ_s/μ ($\mu = \sin^{-1}\frac{1}{M}$) lies between 1.03 and 1.10 in the Mach number range M = 1.4 to 2.8, for these wings with semi-span to length ratios up to 1/3 and thickness chord ratios up to 0.1123. The dependence of θ_s/μ on M for a given wing is almost linear in this range for the single wing for which sufficient data is available (see Fig.2).

It is of some interest that, for these weak shocks, linear theory predicts the pressure rise across the wave quite successfully. According to linear theory, the pressure is continuous across the conical Mach wave attached to the apex but has an infinite pressure gradient there. It predicts a maximum value close to this wave and these maxima have been compared with values calculated from the shock relations, using the measured values of the shock angle, θ_s. In the cases considered, the values computed by linear theory are lower than the corresponding values computed from the measured shock angles, by up to 22%; see Table 1, below. The actual figures are only approximate, since the estimated accuracy in the measurement of the shock angles (±0.1 degree) results in an uncertainty of approximately ±8% in the pressure coefficient.

Table 1

Values of C_p near Mach cone

(Model numbers refer to the R.A.E. 8' x 8' tunnel sequence)

Model No.	Mach number	$C_{P(1)}$	$C_{P(2)}$	Range of $C_{P(2)}$ within accuracy of θ_s	$\frac{C_{P(1)}}{C_{P(2)}}$ (%)
233	2	0.0617	0.0645	0.0618 to 0.0671	96
234	2	0.0463	0.0514	0.0487 to 0.0540	90
239	2.8	0.0341	0.0408	0.0397 to 0.0429	84
242	2.2	0.0236	0.0302	0.0278 to 0.0327	78
242	2.4	0.0235	0.0298	0.0275 to 0.0321	79
242	2.6	0.0234	0.0292	0.0270 to 0.0313	80
242	2.8	0.0233	0.0284	0.0264 to 0.0305	82

Subscripts: (1) Maximum value of C_p near Mach cone, in plane x = 0.6, according to linear theory.

(2) Values computed from measured shock angles.

4.2.2 Trailing edge Mach wave

In Fig.3(a)-(d), pressure distributions along the oentre line of the wing have been plotted for four values of the parameter βs. Linear theory predicts a discontinuity in pressure coeffioient at the trailing edge and the magnitude of this discontinuity has been compared with values calculated from the shock relations using one-half the centre line trailing edge angle as the defleotion angle. This angle, 6, is given by ten $\delta = \frac{0.5}{s}(c_0 + c_1 + c_2 + c_3)$, = $\frac{0.125\ c_0}{s}$ for the Lord V area distribution. In the present case $c_0 = 0.28$, so $\delta = 6.65^\circ$ and 3.08° for $s = 1/3$ ard 0.65 respectively. The local Mach number ahead of this shook is calculated *from* the pressure coefficient predicted by linear theory and, for comparison, also taken to be equal to the free stream Mach number. The first of these methods predicts local Mach numbers which are 4% to 8½% above the free stream value in the cases considered.

Fig.3 shows that the jump predioted by linearized theory is very close to that calculated from the shock relations, using the local value of the upstream Mach number. The maximum error in four cases is only 11,.. Bi6ger discrepances (Up to 34%) arise if the free stream Mach number is used.

All three predictions of the pressure jump across the trailing edge show that the pressure rises from a value below free stream to a value well above it.

This may be compared with earlier investigations made by various authors[10,11,12]. They calculated the local flow direotion along the oentre line of the (linearized) wake of a flat-plate delta or rectangular wing at incidence. In the case of a lifting wing without thiokneas, the pressure in the wake returns to its free stream value immediately downstream of the trailing edge, with a subsequent adjustment of the flow direction to a downstream asymptotio value. In the present case the flow in the wake returns to the free stream direction immediately downstream of the trailing edge, with a subsequent adjustment of the pressure to the free stream value. In each case there is an over-adjustment beyond the ultimate downstream value ad, in eaoh case, this decays very rapidly. (Compare Fig.3 with Fig.1 of Ref.10.) In the cases considered here, for example, the pressure coefficient has decayed to values which are less than 0.003 one chord length behind the wing (i.e. $x = 2$), and less then 0.0001 another half-chord length downstream ($x = 2.5$).

In the real flow, the shook wave will attenuate with increasing distance from the wing. Linear theory predicts a plane Mach wave of constant strength, making a constant angle with the free stream direction, and occupying the strip $|y| \leq s$ of the plane $z = (x-1)/\beta$. The strengths of both the shock and the Mach wave vary across the span (since the trailing edge angle varies linearly across the span).

4.3 Discussion of the charts

The main body of the results consists of charts of contours, along each of which one of the three components of the perturbation velocity is constant. Each chart is for a particular plane perpendicular to the free stream direction. The region covered is restricted to the positive quadrant ($y, z \geq 0$); this is sufficient owing to the symmetry of the functions about the planes $y = 0$ and $z = 0$. Two delta wings, each of "Lord V" area distribution, but of differing planform geometry ($s = 1/3$ and 0.65), have been considered. For the Lord V distribution, the values of the coefficients c_0, c_1, c_2, c_3 (which appear in Section 3) are given by $c_0 : c_1 : c_2 : c_3 = 4 : -6 : 4 : -1$. The cross-sectional area distribution is given, therefore, by

$$S(x) = 2s \times z(x,0)$$

$$= c_0 x^2 (1 - x)(1 - 1.5x + x^2 - 0.25x^3) ,$$

where c_0 is taken as $c_0 = 0.28$ in the present case.

It can be shown that the thickness/chord ratio (t/c) is given by

$$t/c = 0.43375 c_0/s , = 0.03745/s \text{ in the present case.}$$

It follows that $t/c = 0.1123$ and 0.0576 for $s = 1/3$ and 0.65, respectively. (See *Figs.2 and* 3 of Ref.4 for illustrations of the Lord V centre-section and cross-sectional area distributions.) Results are given for a plane just ahead of the trailing edge (for which $x = 0.9999$) for three Mach numbers ($M = 1.6$, 2.2 and 3) for the first wing, and for a single Mach number ($M = 1.6$) for the second wing. This provides results in this plane for four values of the parameter βs (0.41633, 0.65320, 0.81185 and 0.94281). Charts are also given representing velocities in the planes $x = 2$ and 3 for the smallest of the four values of βs mentioned above (corresponding to $M = 1.6$, $s = 1/3$).

To the aoouraoy of linear theory, the pressure *coefficient is given* by $C_p = -\frac{2}{U}\frac{\partial \phi}{\partial x}$. It follows that any curve on which the streamwise velocity component is constant is also an isobar. These curves are each labelled with a particular value of C_p, scaled by a factor 100, for convenience. (Hence the isobar on which $C_p = -0.03$ is labelled "-3".) The other two sets of curves are labelled similarly, by values of the functions $-\frac{200}{U}\frac{\partial \phi}{\partial y}$ and $-\frac{200}{U}\frac{\partial \phi}{\partial z}$.

The characteristics of these three sets of ourvea are described in Sections *4.3.1, 4.3.2 and* 4.3.3, for the streamwise, transverse and vertical components of velocity, respectively.

4.3.1 Streamwise component of velocity

Figs.4-7 contain isobars in the plane x = 0.9999 for four different values of βs; *Figs.8 and 9* contain curves corresponding to the planes x = 2 *and 3* respectively for the case βs = *0.41633. For x = 0.9999 (just on the* wing), the isobars cut the planes y = 0 and z = 0 normally except across the plane of the wing (a = 0, $|y| \leq s$). They are approximately circular in shape in the region of $r(=\beta\sqrt{y^2 + z^2}/x) = 0.8$, but become more elliptical nearer the wing. The maximum and minimum values of C_p, (denoted $C_{P(max)}$ and $C_{P(min)}$), for a given wing and Mach number, both occur on the line x = 0.9999, z = 0, off and on the wing respectively. These two functions are plotted in Fig.10 against the parameter $\eta = (1 - \beta^2 s^2)^{-\frac{1}{2}}$. This parameter is used as $C_{P(max)}$ is approximately a linear function of it in the range considered. The maximum value on the line x = 0.9999, y = 0 varies very little with η, but is lower in all oases than the maximum on the line x = 0.9999, z = 0. This causes one or more of the isobars to contain a loop, beginning and ending on the line *x = 0.9999,* z = 0 (e.g. the isobar on which C_p = 0.05, in Fig.4).

Near the Mach cone and behind the trailing edge, the curves are approximately circular, as for x < 1, and the maximum value of C_p which occurs in this region decreases as x increases. A similar behaviour would result from the attenuation of the bow shock wave in the real flow. There is a discontinuity in the pressure coefficient across the strip $|y| \leq s$ of the plane $z = (x-1)/\beta$. The magnitude of this discontinuity on the centre line of the wing has been disoussed earlier (Section 4.2). It falls off linearly (to zero) as y increases, from zero, to the value y = a.

4.3.2 Transverse component of velocity

The level ourvea of the function $-\frac{200}{U}\frac{\partial\phi}{\partial y}$ are given in Figs.11-16. Ahead of the trailing edge (x = 0.9999), the quadrant is separated into two regions by a more or less circular curve given by $\frac{\partial\phi}{\partial y} = 0$ (the "zero ourve"). Along this r varies between 0.60 and 0.75 in the oases considered here. This is the only curve which intersects the line x = 0.9999, y = 0 since $\frac{\partial\phi}{\partial y} = 0$ everywhere on thia line, from symmetry. Outside of the "zero curve" the aouroea at the front of the wing dominate, and behind it the sinks, which lie behind the line of greatest thickness of the wing, have the greater effect. On the zero curve the contributions of the two just balance. All the other curves begin and end on the line x = 0.9999, z = 0. $\frac{\partial\phi}{\partial y}$ is negative inside

the 'zero curve' and positive outside. Along the line $x = 0.9999$, $z = 0$, $\frac{\partial\phi}{\partial y}$ decreases (from zero) to a negative minimum in the region of $\frac{y}{s} = 0.6$ and then increases to a positive maximum near the Mach cone. These turning values, scaled by the factor a, are plotted against the parameter η in Fig.17. It will be seen that the function $\left[-\frac{2}{U} s \frac{\partial\phi}{\partial y}\right]_{max}$ is almost independent of η (about 0.04), whereas $\left[-\frac{2}{U} s\frac{\partial\phi}{\partial y}\right]_{min}$ decreases fairly linearly with η.

For $x > 1$, there are two curves on which $\frac{\partial\phi}{\partial y} = 0$, both of which are more or leas circular. On the outer one $r \simeq 0.81$ and 0.88 for $x = 2$ and 3, respectively, and on the inner one $r \simeq (x-1)/\beta$. Between the Mach cone and the outer zero curve, $\frac{\partial\phi}{\partial y}$ is positive, as for the case $x < 1$, ad negative between the two curves. Inside the inner "zero curve", $\frac{\partial\phi}{\partial y}$ takes small positive values, leas than 0.005 in the two oases considered. Along the plane Mach wave from the wing trailing edge ($|y| \leq a$, $z = (x-1)/\beta$), the level curves have discontinuities in gradient.

4.3.3 Vertical component of velocity

The level curves of the function $-\frac{200}{U}\frac{\partial\phi}{\partial z}$ are given in Figs.18-23. One basic feature of these curves results from the boundary conditions (given in equations (2) and (3)). $\frac{\partial\phi}{\partial z}$ increases linearly along the line $x = 0.9999$, $z = 0$, from its negative minimum at $y = 0$ to zero at the point $y = s$, and remains zero at all points off the wing. For $x = 0.9999$, there is a "zero curve", which intersects the line $z = 0$ where $y \geq sx$. Between this curve and the Mach cone the behaviour is similar to that described for the transverse component except that the roles of the planes $y = 0$ and $z = 0$ are reversed. Inside the "zero curve", $\frac{\partial\phi}{\partial z}$ is negative and each curve intersects both of the lines $x = 0.9999$, $z = 0$ and $x = 0.9999$, $y = 0$, the latter normally. The minimum value of $\frac{\partial\phi}{\partial z}$ occurs at the origin, where $\frac{200}{U}\frac{\partial\phi}{\partial z} = -100\,(c_0 + c_1 + c_2 + c_3)/s, = -7/s$ in the present case. The maximum value of $\frac{\partial\phi}{\partial z}$ occurs on the line $x = 0.9999$, $y = 0$ except for the case in which $M = 3$, when a small closed contour exists in the region of $y = 0.26$, $z = 0.21$ (see Fig.20). In this case the maximum value lies inside this contour.

For $x > 1$, there are two "zero curves", as for the functions. Between the outer curve and the Mach cone the features are similar to those described for the case $x < 1$. There is a discontinuity in $\frac{\partial\phi}{\partial z}$ at the same position as that in the pressure coefficient (where $z = (x-1)/\beta$) and the behaviour for smaller values of z is similar to that of the pressure coefficient, as its value falls rapidly towards the plane of the wing.

5 CONCLUSIONS

The velocity field about a family of symmetrical delta wings at sero incidence in a supersonic stream has been calculated by linearized theory. Closed-form expressions for the three components of the perturbation velocity in terms of elementary functions have been derived, and have been programmed for automatic digital oomputaticn on the Ferranti Mercury computer. The programme has been used to illustrate features of the flow field of a "Lord V" wing having rhcmic orcss-sections normal. to the free stream direoticn, for four values of the similarity parameter βs. The main results are presented as contours of the velocity components in planes normal to the free stream direction, at and behind the wing *trailing edge.*

The pressure coefficient predicted by linear theory rises to a maximum value a short distance behind the Mach cone from the apex. This *maximum* value has been compared with values calculated by the shock relations from measured values of the shock wave angle for wings with thickness-chord ratios of 0.0643 and 0.1123. It is found that linear theory somewhat urdereatimates this pressure coefficient. The discontinuity in pressure on the oentre-line of the wing which occurs at the trailing edge has been compared with values calculated from the shock relations. Good agreement is found.

Appendix A

VALUES OF X-COORDINATES AND THEIR DERIVATIVES

The values of the x-coordinates which appear in the integral limits in equation (5) and/or (5A) have the following values:

$$\left.\begin{aligned} x_A &= [(x+\beta^2\, sy) - \sqrt{(x+\beta^2\, sy)^2 - (1-\beta^2\, s^2)\,(x^2-\beta^2\, y^2-\beta^2\, z^2)}]/(1-\beta^2\, s^2) \\ x_B &= x - \beta\sqrt{y^2+z^2} \\ x_C &= x - \beta z \\ x_D &= [(x-\beta^2\, sy) - \sqrt{(x-\beta^2\, sy)^2 - (1-\beta^2\, s^2)\,(x^2-\beta^2\, y^2-\beta^2\, z^2)}]/(1-\beta^2\, s^2) \\ x_M &= \begin{cases} x_C \text{ if } x-\beta z > y/s \\ x_D \text{ if } x-\beta z \leq y/s \end{cases} \end{aligned}\right\} \quad (A1)$$

The derivatives of $\tilde{x}_M$ and $\tilde{x}_D$ appear in the expressions for the velocity components, given in equations (11)-(13).

We have

$$\left.\begin{aligned} \frac{\partial x_C}{\partial x} &= 1 \\ \frac{\partial x_C}{\partial y} &= 0 \\ \frac{\partial x_C}{\partial z} &= -\beta \end{aligned}\right\} \quad (A2)$$

$$\left.\begin{aligned} \frac{\partial x_D}{\partial x} &= \left[\frac{(x - x_D)}{(x - \beta^2\, sy) - (1 - \beta^2\, s^2)\, x_D}\right] \\ \frac{\partial x_D}{\partial y} &= \left[\frac{\beta^2\,(s\, x_D - y)}{(x - \beta^2\, sy) - (1 - \beta^2\, s^2)\, x_D}\right] \\ \frac{\partial x_D}{\partial z} &= \left[\frac{-\beta^2\, z}{(x - \beta^2\, sy) - (1 - \beta^2\, s^2)\, x_D}\right] \end{aligned}\right\} \quad (A3)$$

Appendix B

VALUES OF THE FUNCTIONS B_N

These functions appear in equation (9) and have the following values:

$$B_1 = \left\{ \frac{h(x')}{\beta^2 s} \sqrt{(x-x')^2 - \beta^2 y^2 - \beta^2 z^2} - \frac{1}{\beta} \left[g(x') - \frac{y}{s} h(x') \right] \sin^{-1} \left(\frac{\beta y}{\sqrt{(x-x')^2 - \beta^2 z^2}} \right) \right\}$$

$$B_2 = \left\{ \frac{h(x')}{\beta^2 s} \sqrt{(x-x')^2 - \beta^2 (y+sx')^2 - \beta^2 z^2} - \frac{1}{\beta} \left[g(x') - \frac{y}{s} h(x') \right] \sin^{-1} \left(\frac{\beta(y+sx')}{\sqrt{(x-x')^2 - \beta^2 z^2}} \right) \right\}$$

$$B_3 = \left\{ - \frac{1}{\beta} \left[g(x') - \frac{y}{s} h(x') \right] \frac{\pi}{2} \right\}$$

$$B_4 = \left\{ - \frac{h(x')}{\beta^2 s} \sqrt{(x-x')^2 - \beta^2 y^2 - \beta^2 z^2} - \frac{1}{\beta} \left[g(x') + \frac{y}{s} h(x') \right] \sin^{-1} \left(\frac{\beta y}{\sqrt{(x-x')^2 - \beta^2 z^2}} \right) \right\}$$

$$B_5 = \left\{ - \frac{h(x')}{\beta^2 s} \sqrt{(x-x')^2 - \beta^2 (y-sx')^2 - \beta^2 z^2} - \frac{1}{\beta} \left[g(x') + \frac{y}{s} h(x') \right] \sin^{-1} \left(\frac{\beta(y-sx')}{\sqrt{(x-x')^2 - \beta^2 z^2}} \right) \right\}$$

$$B_6 = \left\{ - \frac{1}{\beta} \left[g(x') + \frac{y}{s} h(x') \right] \left(- \frac{\pi}{2} \right) \right\}$$

$$B_7 = \left\{ - \frac{1}{\beta} \left[g(x') + \frac{y}{s} h(x') \right] \left(\frac{\pi}{2} \right) \right\} = - B_6$$

Appendix C

CLASSIFICATION OF INTEGRALS

The following integrals occur in the expressions for the velocity components:

$$G_N = \int_0^{\tilde{x}_B} \left\{ \frac{(x-x')\, x'^N \sqrt{(x-x')^2 - \beta^2 y^2 - \beta^2 z^2}}{[(x-x')^2 - \beta^2 z^2]} \right\} dx' \qquad N=0(1)3$$

$$G_{N+4} = \int_0^{\tilde{x}_B} \left\{ \frac{x'^N \sqrt{(x-x')^2 - \beta^2 y^2 - \beta^2 z^2}}{[(x-x')^2 - \beta^2 z^2]} \right\} dx' \qquad N=0(1)3$$

$$H_{N+10} = \int_0^{\tilde{x}_B} \left\{ \frac{(x-x')\, x'^N}{[(x-x')^2 - \beta^2 z^2] \sqrt{(x-x')^2 - \beta^2 y^2 - \beta^2 z^2}} \right\} dx' \qquad N=0(1)4$$

$$V_N = \int_0^{x_A} \frac{x'^N\, dx'}{\sqrt{(x-x')^2 - \beta^2 (y+sx')^2 - \beta^2 z^2}} \qquad N=0(1)4$$

$$Z_N = \int_0^{\tilde{x}_A} \frac{x-x'\quad x'^N\, dx'}{[(x-x')^2 - \beta^2 z^2] \sqrt{(x-x')^2 - \beta^2} \sqrt{(y+sx')^2 - \beta^2 z^2}} \qquad N=0(1)5$$

$$Y_{N+160} = \int_0^{x_A} \frac{x'^N\, dx'}{[(x-x')^2 - \beta^2 z^2 I \sqrt{(x-x')^2 - \beta^2 (y+sx')^2 - \beta^2 z^2}} \qquad N=0(1)5$$

$$U_N = \int_0^{\tilde{x}_D} \frac{x'^N\, dx'}{\sqrt{(x-x')^2 - \beta^2 (y-sx')^2 - \beta^2 z^2}} \qquad N=0(1)4$$

$$W_N = \int_0^{\tilde{x}_D} \frac{(x-x')\, x'^N\, dx'}{[(x-x')^2 - \beta^2 z^2] \sqrt{(x-x')^2 - \beta^2 (y-sx')^2 - \beta^2 z^2}} \qquad N=0(1)5$$

$$Y_{N+60} = \int_0^{\tilde{x}_D} \frac{x'^N \, dx'}{[(x-x')^2 + \beta^2 z^2] \sqrt{(x-x')^2 + \beta^2 (y-ax')^2 + \beta^2 z^2}} \qquad N=0(1)5$$

The following integrals occur in the solution of the above:

$$C_N = \int_{\theta_o}^{\theta_1} \cosh^N \theta \, d\theta \qquad N=0(1)4$$

$$D_N = \int_{\psi_o}^{\psi_1} \cosh^N \psi \, d\psi \qquad N=0(1)4$$

$$E_N = \int_{\phi_o}^{\phi_1} \cosh^N \phi \, d\phi \qquad N=0(1)4$$

$$F_N = \int_{\phi_\theta}^{\phi_1} \frac{\cosh^N \phi \, d\phi}{y^2 \cosh^2 \phi + z^2 \sinh^2 \phi} \qquad N=0(1)6$$

Appendix D

EVALUATION OF THE INTEGRALS LISTED IN APPENDIX C

D.1 C_N, D_N, E_N, F_N

The first three integrals are identical except for the limits of integration, which are given by

$$\cosh\ \theta_1 = \left(\frac{a_1}{a_1 - x_D}\right), \quad \cosh\ \theta_o = \left(\frac{a_1 - \tilde{x}_D}{a_1 - x_D}\right) \quad \text{where} \quad a_1 = \frac{x - \beta^2 sy}{1 - \beta^2 s^2}$$

$$\text{cash}\ \psi_1 = \left(\frac{a_2}{a_2 - x_A}\right), \quad \cosh\ \psi_o = \left(\frac{a_2 - x_A}{a_2 - x_A}\right) \quad \text{where} \quad a_2 = \frac{x + \beta^2 sy}{1 - \beta^2 s^2}$$

$$\text{oosh}\ \phi_1 = \left(\frac{x}{\beta\sqrt{y^2 + z^2}}\right), \quad \cosh\ \phi_o = \left(\frac{x - \tilde{x}_B}{\beta\sqrt{y^2 + z^2}}\right) .$$

We have

$$C_0 = [\theta]_{\theta_o}^{\theta_1}$$

$$C_1 = [\sinh\ \theta]_{\theta_o}^{\theta_1}$$

$$C_2 = [\tfrac{1}{2}\ \theta + \tfrac{1}{2}\ \sinh\ \theta\ \cosh\ \theta]_{\theta_0}^{\theta_1}$$

$$C_3 = [\sinh\ \theta + \tfrac{1}{3}\ \sinh^3\ \theta]_{\theta_o}^{\theta_1}$$

$$C_4 = [\tfrac{3}{8}\ \theta + \tfrac{1}{2}\ \sinh\ \theta\ \cosh\ \theta + \tfrac{1}{8}\ \sinh^3\ \theta\ \cosh\ \theta + \tfrac{1}{8}\ \sinh\ \theta\ \cosh^3\ \theta]_{\theta_0}^{\theta_1}$$

and similarly for D_N and E_N in terms of ψ and ϕ respectively.

We oan obtain the following reduotion formula for F_N:

$$F_N = \left(\frac{z^2 F_{N-2} + E_{N-2}}{y^2 + z^2} \right) \quad ,$$

where

$$F_0 = \begin{cases} \frac{1}{yz} \left[\tan^{-1} \left(\frac{z \tanh \phi}{y} \right) \right]_{\phi_o}^{\phi_1} & \text{for } z \neq 0 \\ \frac{1}{y^2} \left[\tanh \phi \right]_{\phi_o}^{\phi_1} & \text{for } z = 0 \end{cases}$$

$$F_1 = \frac{1}{y\sqrt{y^2 + z^2}} \left[\tan^{-1} \left(\frac{\sqrt{y^2 + z^2} \sinh \phi}{y} \right) \right]_{\phi_o}^{\phi_1} \quad .$$

The **case** y = 0 has been speoifioally **excluded;** sufficiently accurate values may be obtained by using a very small value for y in the computer **programme** (say y = 0.00001).

D.2 G_N, $G_{(N+4)}$, $H_{(N+10)}$

These integrals **are** transformed by the substitution

$$x - x' = \beta \sqrt{y^2 + z^2} \cosh \phi \quad .$$

It follows that:

$$G_0 = \beta (y^2 + z^2)^{3/2} (F_3 - F_1)$$

$$G_1 = x G_0 - \beta^2 (y^2 + z^2)^2 (F_4 - F_2)$$

$$G_2 = - x^2 G_0 + 2x G_1 + \beta^3 (y^2 + z^2)^{5/2} (F_5 - F_3)$$

$$G_3 = x^3 G_0 - 3x^2 G_1 + 3x G_2 - \beta^4 (y^2 + z^2)^3 (F_6 - F_4)$$

$$G_4 = (y^2 + z^2)(F_2 - F_C)$$

$$G_5 = x\,G_4 - \beta (y^2 + z^2)^{3/2} (F_3 - F_1)$$

$$G_6 = -x^2 G_4 + 2x\,G_5 + \beta^2 (y^2 + z^2)^2 (F_4 - F_2)$$

$$G_7 = x^3 G_4 - 3x^2 G_5 + 3x\,G_6 - \beta^3 (y^2 + z^2)^{5/2} (F_5 - F_3)$$

$$H_{10} = F_1 \sqrt{y^2 + z^2}/\beta$$

$$H_{11} = x\,H_{10} - (y^2 + z^2) F_2$$

$$H_{12} = -x^2 H_{10} + 2x\,H_{11} + \beta (y^2 + z^2)^{3/2} F_3$$

$$H_{13} = x^3 H_{10} - 3x^2 H_{11} + 3x H_{12} - \beta^2 (y^2 + z^2)^2 F_4$$

$$H_{14} = -x^4 H_{10} + 4x^3 H_{11} - 6x^2 H_{12} + 4x H_{13} + \beta^3 (y^2 + z^2)^{5/2} F_5$$

D.3 V_N, Z_N, Y_{N+160}

The substitution used in these integrals is

$$x' = a_2 + (x_A - a_2) \operatorname{oosh} \psi \ .$$

We can show that

$$\sqrt{(x - x')^2 - \beta^2 (y + sx')^2 - \beta^2 z^2} = \sqrt{1 - \beta^2 s^2}\,(a_2 - x_A) \sinh \psi$$

and hence that

$$V_N = \int_{\psi_o}^{\psi_1} \frac{[a_2 + (x_A - a_2) \cosh \psi]^N}{\sqrt{1 - \beta^2 s^2}}\, d\psi \ .$$

It follow that

$$V_N = \frac{1}{\sqrt{1-\beta^2 s^2}}\left\{a_2^N D_o + N a_2^{N-1}(x_A - a_2) D_1 + \ldots + (x_A - a_2)^N D_N\right\} \qquad N=0(1)4$$

Two reduction formulae oan be obtained for the evaluation of Z_N and Y_{N+160}. They are:

$$Y_{N+161} = x\, Y_{N+160} - Z_N$$

$$Z_{N+1} = x\, Z_N - V_N - \beta^2 z^2\, Y_{N+160} .$$

Since the V_N are known, these integrals can be evaluated if Z_0 and Y_{160} are known. In terms of the variable ψ, we have

$$Z_0 = \frac{1}{\sqrt{1-\beta^2 s^2}} \int_{\psi_0}^{\psi_1} \left\{\frac{[x-a_2 + (a_2-x_A)\cosh\psi]}{[x-a_2 + (a_2-x_A)\cosh\psi]^2 - \beta^2 z^2}\right\} d\psi$$

$$Y_{160} = \frac{1}{\sqrt{1-\beta^2 s^2}} \int_{\psi_0}^{\psi_1} \frac{d\psi}{\{[x-a_2 + (a_2-x_A)\cosh\psi]^2 - \beta^2 z^2\}} .$$

It can be shown that

$$Z_0 = \left\{\frac{I(-\beta) + I(+\beta)}{2\sqrt{1-\beta^2 s^2}}\right\}$$

$$Y_{160} = \left\{\frac{I(-\beta) - I(+\beta)}{2\beta z \sqrt{1-\beta^2 s^2}}\right\} .$$

where $I(\pm\beta) = \int_{\psi_0}^{\psi_1} \frac{d\psi}{[x-a_2 \pm \beta z + (a_2-x_A)\cosh\psi]}$.

These integrals can be evaluated using the transformation

$$\tanh \tfrac{1}{2}\psi = \sqrt{\frac{\cosh \psi - 1}{\cosh \psi + 1}}$$

from which it follows that

$$I(+\beta) = \frac{2}{\sqrt{g' h'}} \left[\tan^{-1} \left(\sqrt{\frac{g' (\cosh \psi - 1)}{h' (\cosh \psi + 1)}} \right) \right]_{\psi_0}^{\psi_1}$$

$$I(-\beta) = -\frac{2}{\sqrt{g h}} \left[\tan^{-1} \left(\sqrt{\frac{g (\cosh \psi - 1)}{h (\cosh \psi + 1)}} \right) \right]_{\psi_0}^{\psi_1}$$

where $h = x - x_A - \beta z$

$h' = x - x_A + \beta z$

$g = 2a_2 - x_A - x + \beta z$

$g' = 2a_2 - x_A - x - \beta z$,

all of which are always positive.

D.4 U_N, W_N, Y_{N+60}

The transformation used in the evaluation of these integrals is $x' = a_1 + (x_D - a_1) \cosh \theta$. Since U_N, W_N, Y_{N+60} can be obtained from U_N, Z_N, Y_{N+160}, respectively, by the replacement of "y" by "-y" (see Appendix C), their evaluation is similar to that described in Section D.3. However, the functions ψ, x_A, a_2, D_N are replaced by θ, x_D, a_1, C_N respectively. It should be noted that

$$(1 - \beta^2 s^2)(x_D - a_1) = \sqrt{-(x^2 - \beta^2 sy)^2 - (1 - \beta^2 s^2)(x^2 - \beta^2 y^2 - \beta^2 z^2)}$$

$$= -\beta \sqrt{(y - sx)^2 + (1 - \beta^2 s^2) z^2}$$

For $z = 0$, therefore,

$$(1 - \beta^2 s^2)(x_D - a_1) = -\beta |y - sx| .$$

SYMBOLS

B_N	see equation (9) and Appendix B
c_N	coefficients defining the wing thickness distribution ($N = 0,1,2,3$)
C_P	pressure coefficient
$f(x',y')$	function appearing in equation (5)
$g(x)$, $h(x)$	see equation (7)
M	free stream Mach number
r	$\beta \sqrt{y^2 + z^2}/x$
s	wing semi-spat'
$S(x)$	oross-sectional area at station x
t/c	thickness/chord ratio
U	free stream velooity
x,y,z	right-handed coordinate system, origin 0 at wing apex, Ox along wing centre line, Oyto starboard
x',y',z'	the same when used as running coordinates
x_A, x_B, x_C, x_D, x_M	see Appendix A
Y	value of limit used in equations (8)
$\bar{y}$, $\bar{\bar{y}}$	see equations (5A)
$z(x,y)$	equation of the upper surface of the wing
β	$= \sqrt{M^2 - 1}$.
δ	semi trailing edge angle of wing (on centre line)
η	$= (1 - \beta^2 s^2)^{-1/2}$
θ_s	shock wave angle
λ	see equation (14)
μ	Mach angle, $= \sin^{-1}(1/M)$
τ	area of integration (shown shaded in Fig.1)
ϕ	perturbation velocity potential, in particular on the upper surface of the wing

REFERENCES

No.	Author	Title, etc.
1	W.T. Lord G.G. Brebner	Supersonic flow past narrow wings, with 'similar' cross-sections at zero-lift. Aeron. Quart. IO, 1959, 79-102
2	J. Weber	Some notes on the zero-lift wave drag of slender wings with unswept trailing edges. A.B.C. R & M 3222 December 1959
3	J.H.B. Smith W. Thomson	The calculated effect of the station of maximum cross-sectional area on the wave drag of delta wings. ARC CF.606 September 1961
4	M.C.P. Firmin	The pressure distribution at zero-lift on some slender delta wings at supersonic speeds. ARC CP.774 November 1963
5	J. Weber	Slender delta wings with sharp edges at zero-lift. RAE Technical Note Aero 2508, May 1957 ARC 19,549
6	E. Eminton	Pressure distributions at zero-lift for delta wings with rhombic cross-sections. ARC CP.525 October 1959
7	M.C.P. Firmin	Unpublished Mintech Paper
8	M.C.P. Firmin	Experimental evidence on the drag at zero-lift on a series of slender delta wings at supersonic speeds, and the drag penalty due to distributed roughness. ARC CP.737 February 1963
9	8.0. Ormerod	Private communication, January 1966
10	A. Robinson Sqn. Ldr. J.H. Hunter-Tod	Bound and trailing vortices in linearised theory in supersonic flow, and the downwash in the wake of a delta wing. A.R.C. R & M No.2409, October 1947
11	P.A. Lagerstrom Martha E. Graham	Downwash end sidewash induced by three-dimensional lifting wings in supersonic flow. Douglas Aircraft Co. Report Nc. SM-13007, P.17302, April 1947

REFERENCES (Cont'd)

No.	Author	Title, etc.
12	J.N. Nielsen W.C. Pitts M.P. Gionfriddo	Comparison between theory and experiment for interference pressure field between wing and body at supersonic speeds. NACA Technical Note 3128, April 1954

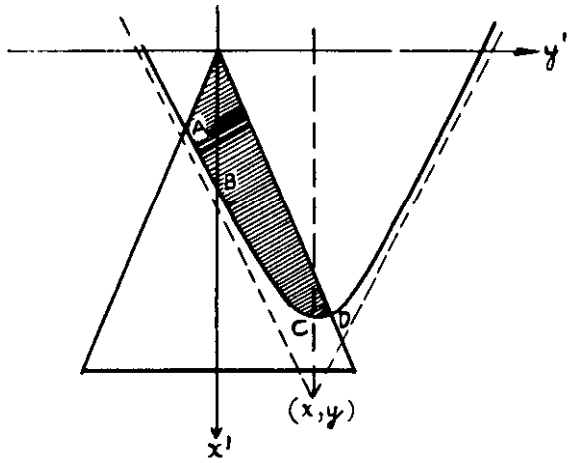

FIG I (a)

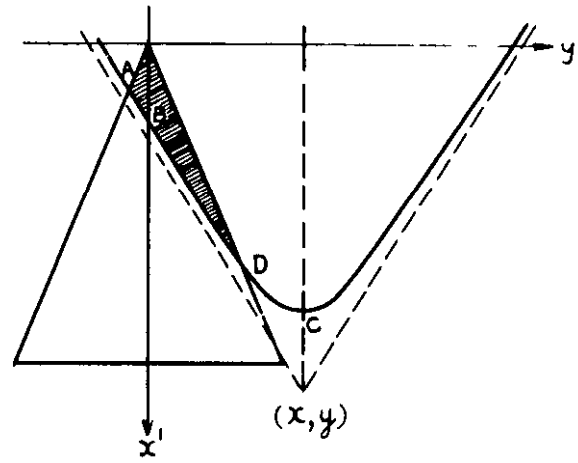

FIG I(b)

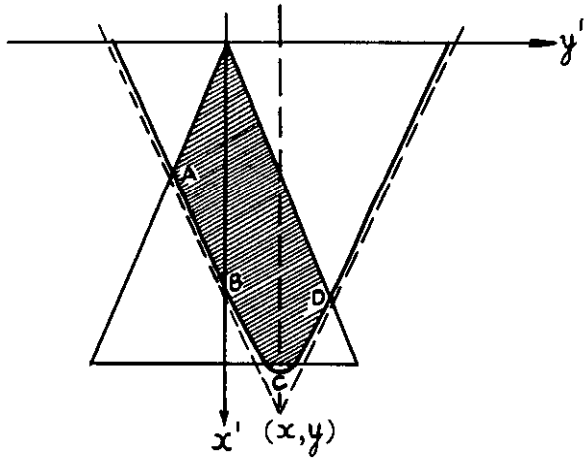

FIG. I (c)

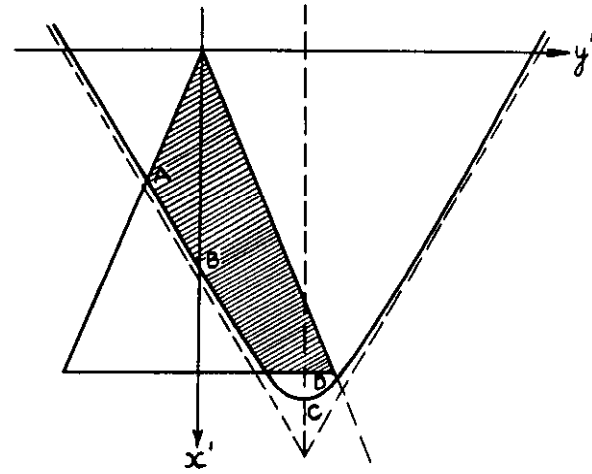

FIG.I (d)

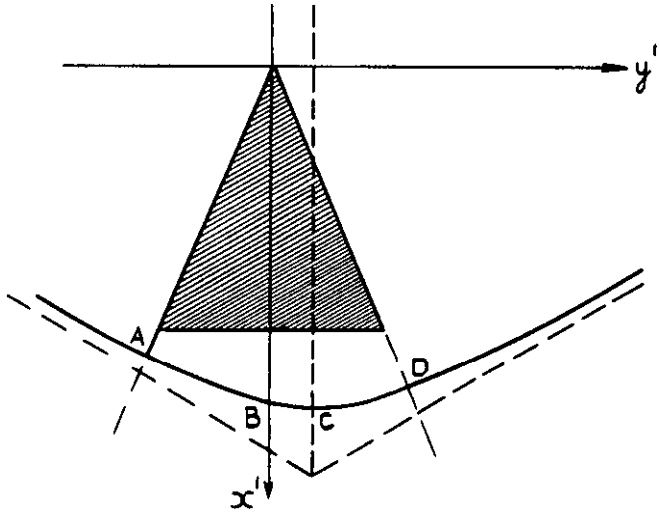

FIG I (e)

FIG	$\tilde{x}_A$	$\tilde{x}_B$	$\tilde{x}_C$	$\tilde{x}_D$	$\tilde{x}_m$
(a)	x_A	x_B	x_C	x_D	x_C
(b)	x_A	x_B	x_C	x_D	x_D
(c)	x_A	x_B	1	x_D	1
(d)	x_A	x_B	1	1	1
(e)	1	1	1	1	1

FIG I PLAN VIEW OF DELTA WING, SHOWING AREA OF INTEGRATION, τ (SHADED), FOR DIFFERENT RELATIVE POSITIONS OF THE WING & THE HYPERBOLA,ABCD

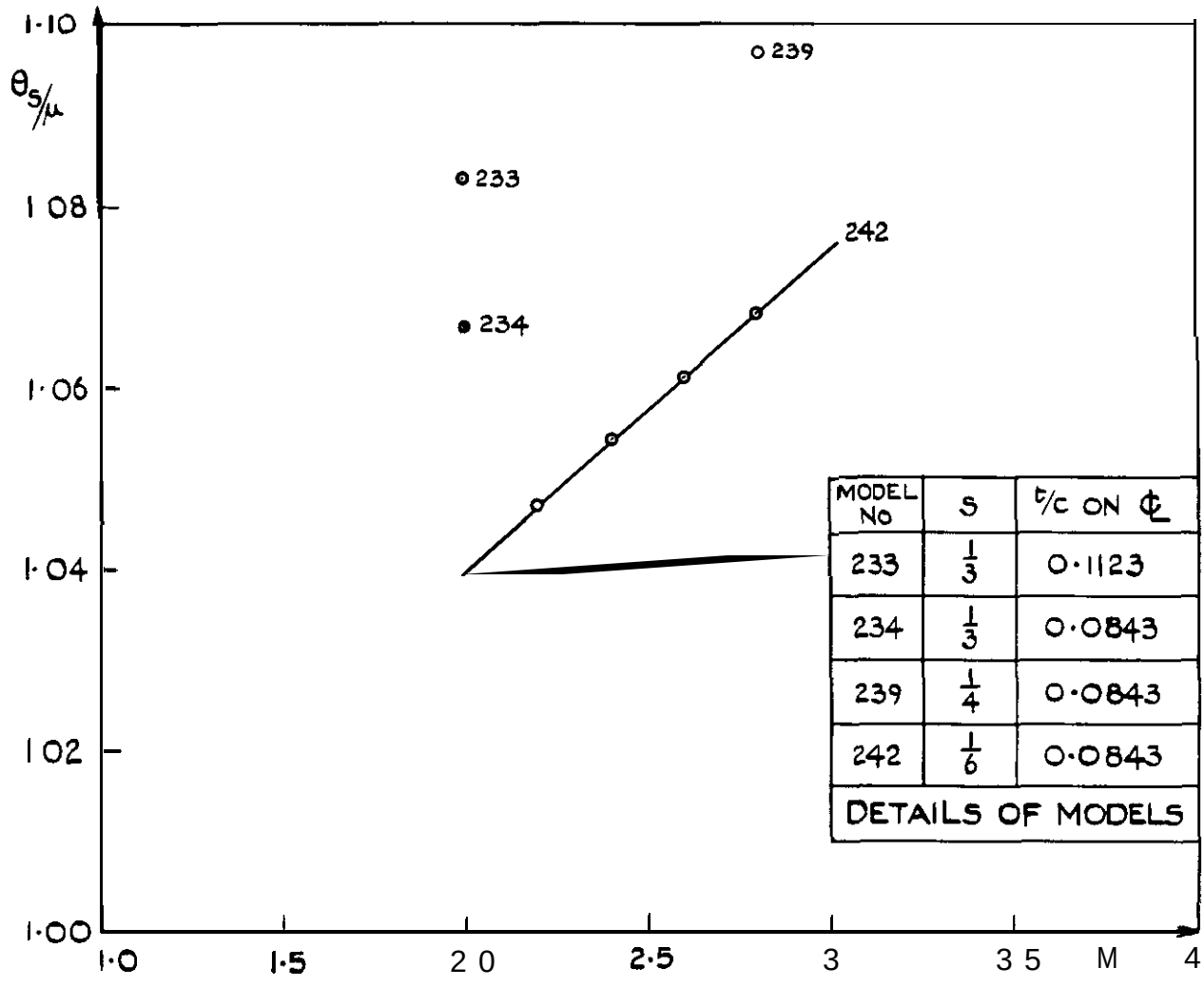

FIG.2 VALUES OF THE FUNCTION θ_s/μ

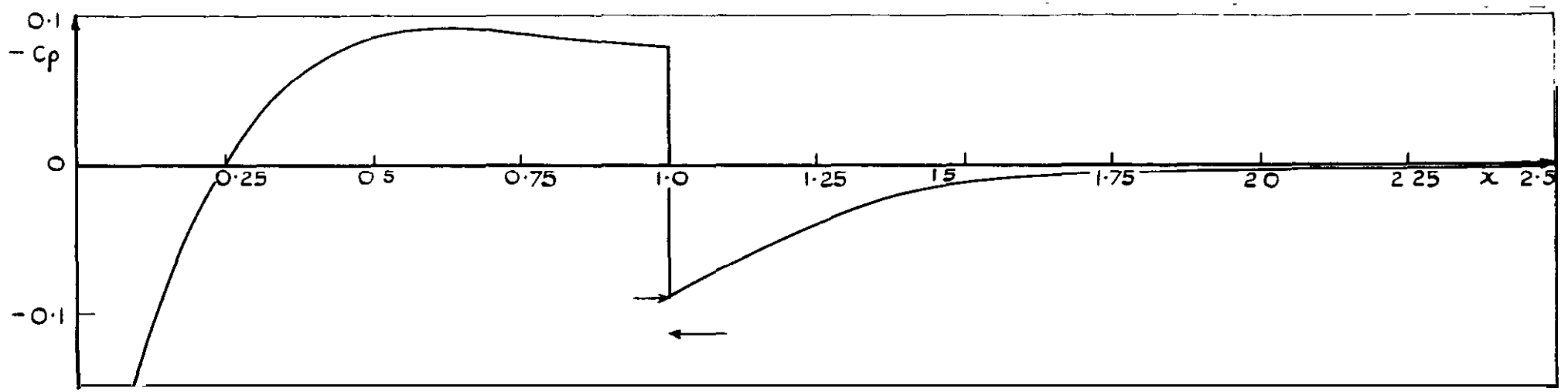

FIG. 3 (a) S= 1/3, M=1·6; βS=0·41633

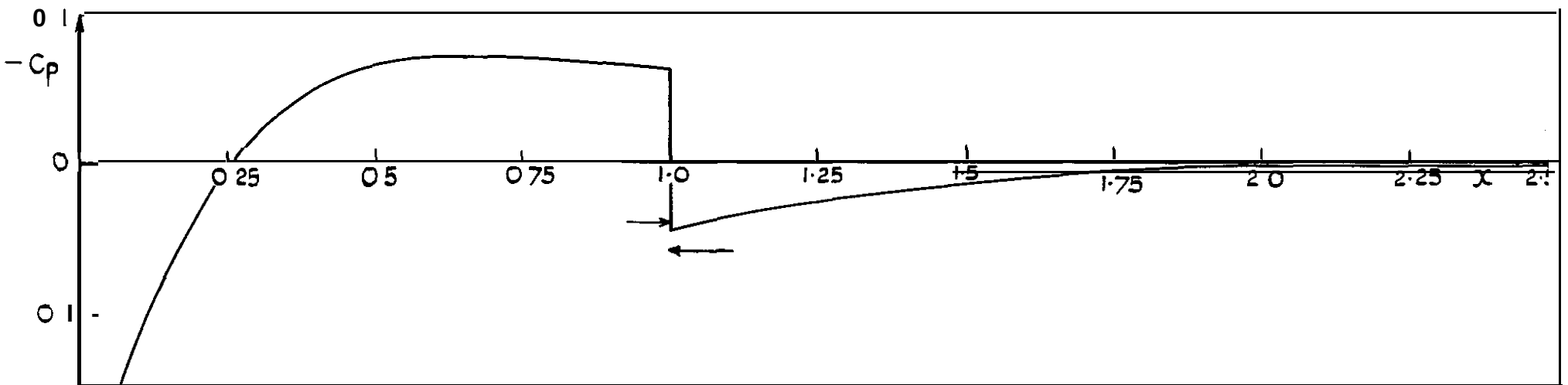

SYMBOL	VALUE TAKEN FOR MACH NUMBER AHEAD OF SHOCK
→	CALCULATED FROM LINEAR PRESSURE COEFFICIENT
←	FREE STREAM VALUE

FIG 3 (b) S=1/3, M=2·2; βS=0·65320

FIG 3 PRESSURE DISTRIBUTION ON THE CENTRE-LINE OF A DELTA WING. OF LORD $\overline{\text{V}}$ AREA DISTRIBUTION

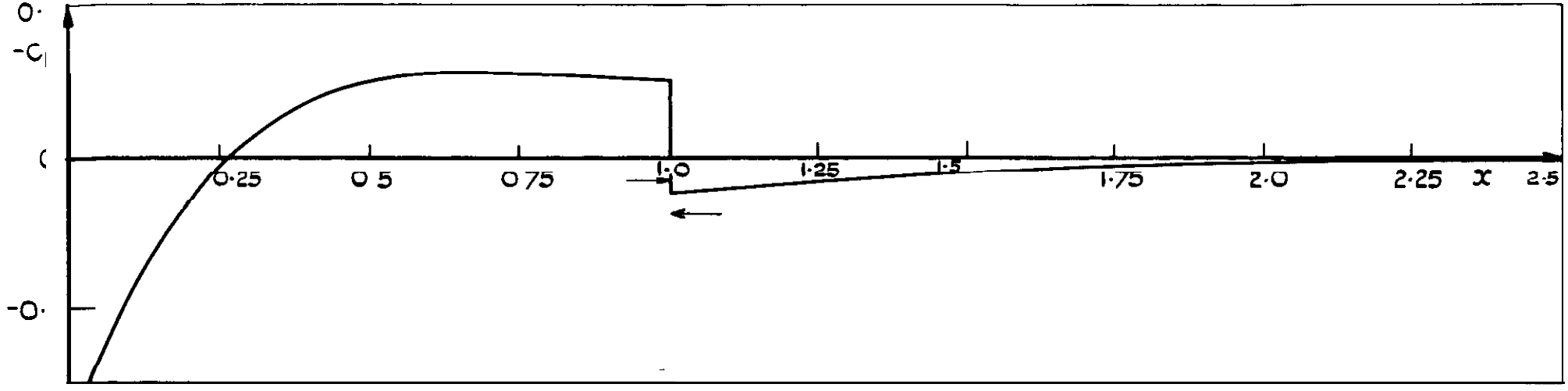

FIG.3 (c) S=1/3, M=3; βS=0·94281

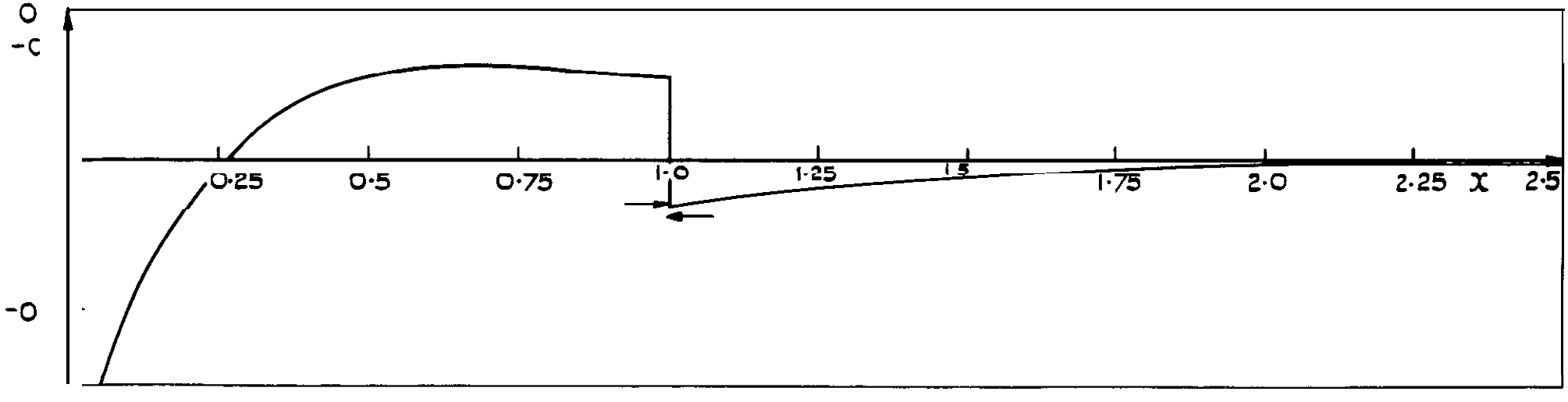

FIG.3 (d) S=0·65, M=1·6; βS=0·81185

IG. 3 (CONT'D) PRESSURE DISTRIBUTION O N THE CENTRE-LINE OF A DELTA WING, OF LORD V AREA DISTRIBUTION

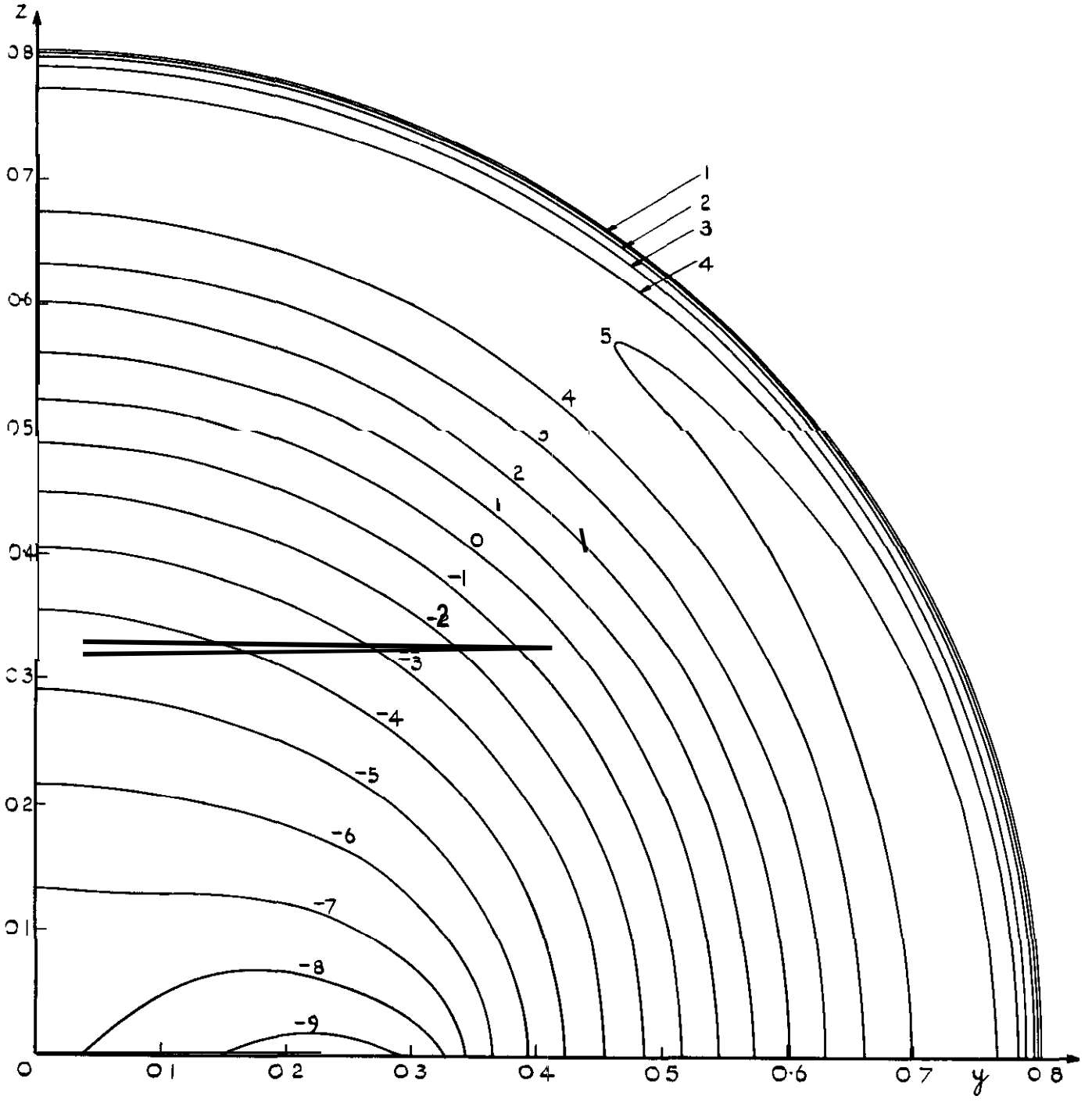

FIG. 4 ISOBARS IN THE PLANE X= 0.9999;
S - f , M=1·6 ; β_S=0·41633

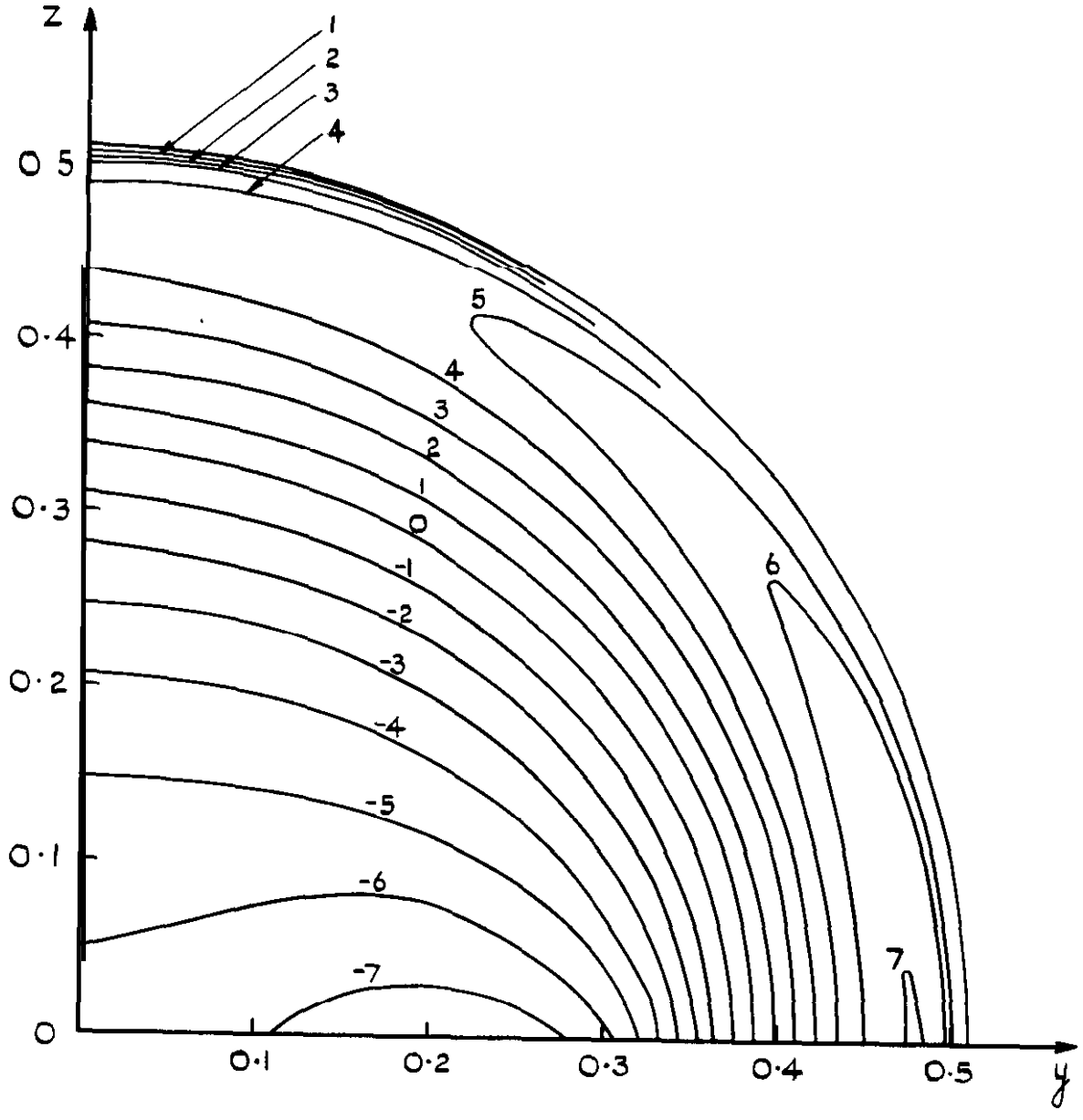

FIG.5 ISOBARS IN THE PLANE X= 0·9999 ;
S = $\frac{1}{3}$, M= 2·2 , βs=0·65320

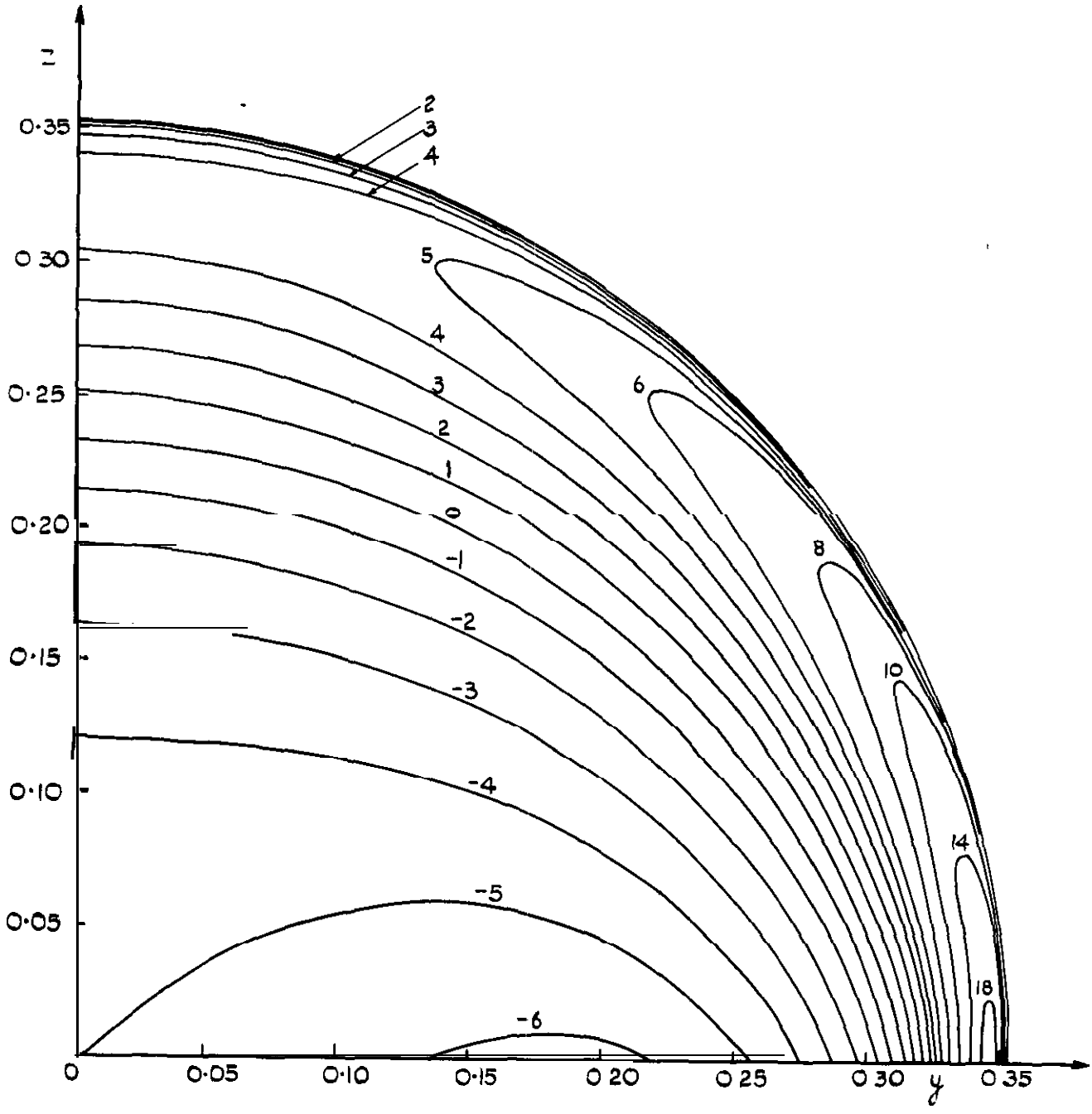

FIG.6 ISOBARS IN THE PLANE $X = 0{\cdot}9999$;
$S = \frac{1}{3}$, $M = 3$; $\beta s = 0{\cdot}94281$

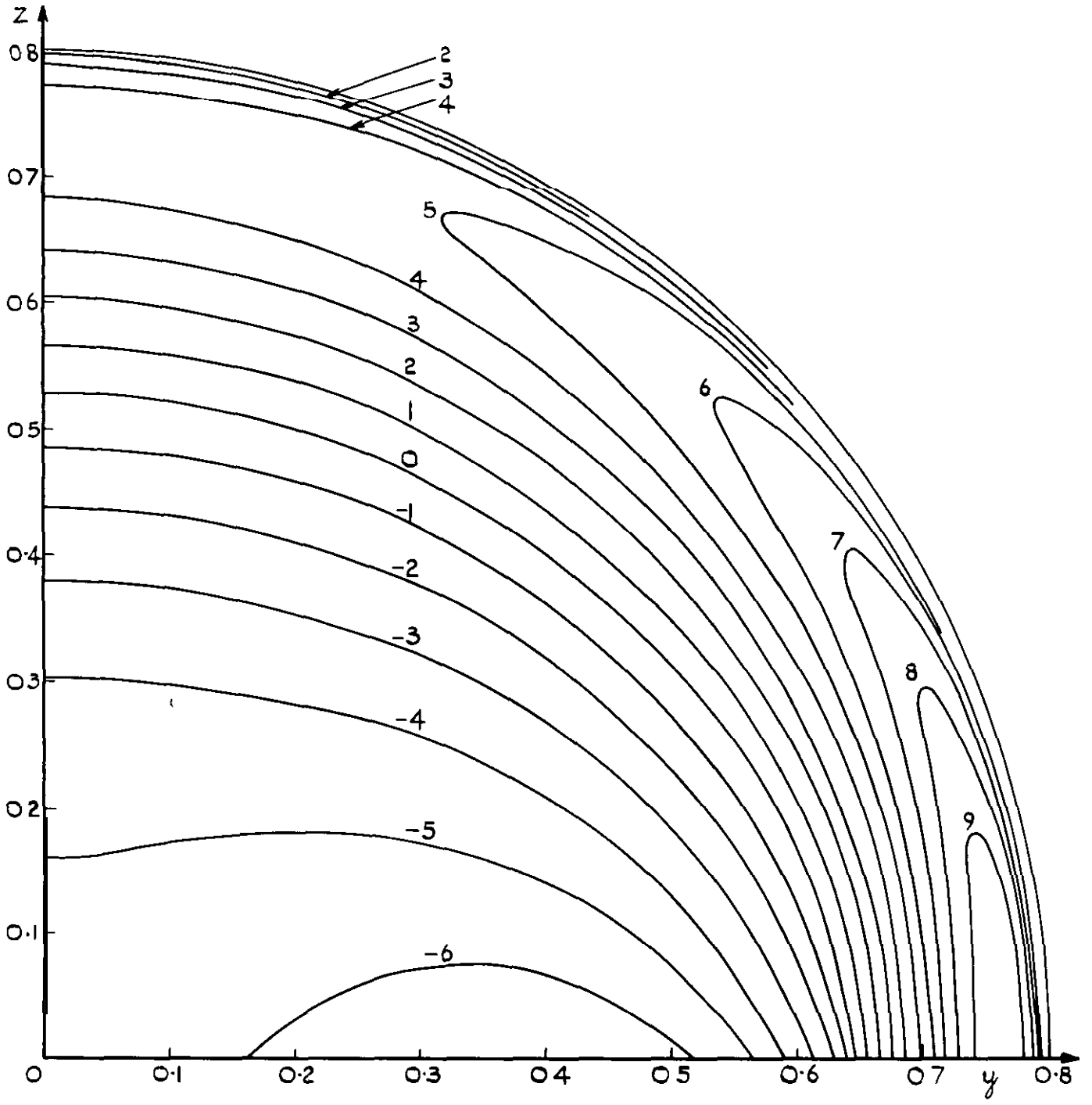

FIG. 7 ISOBARS IN THE PLANE X=0·9999;
S=0·65, M=1·6; βs=0· 81185

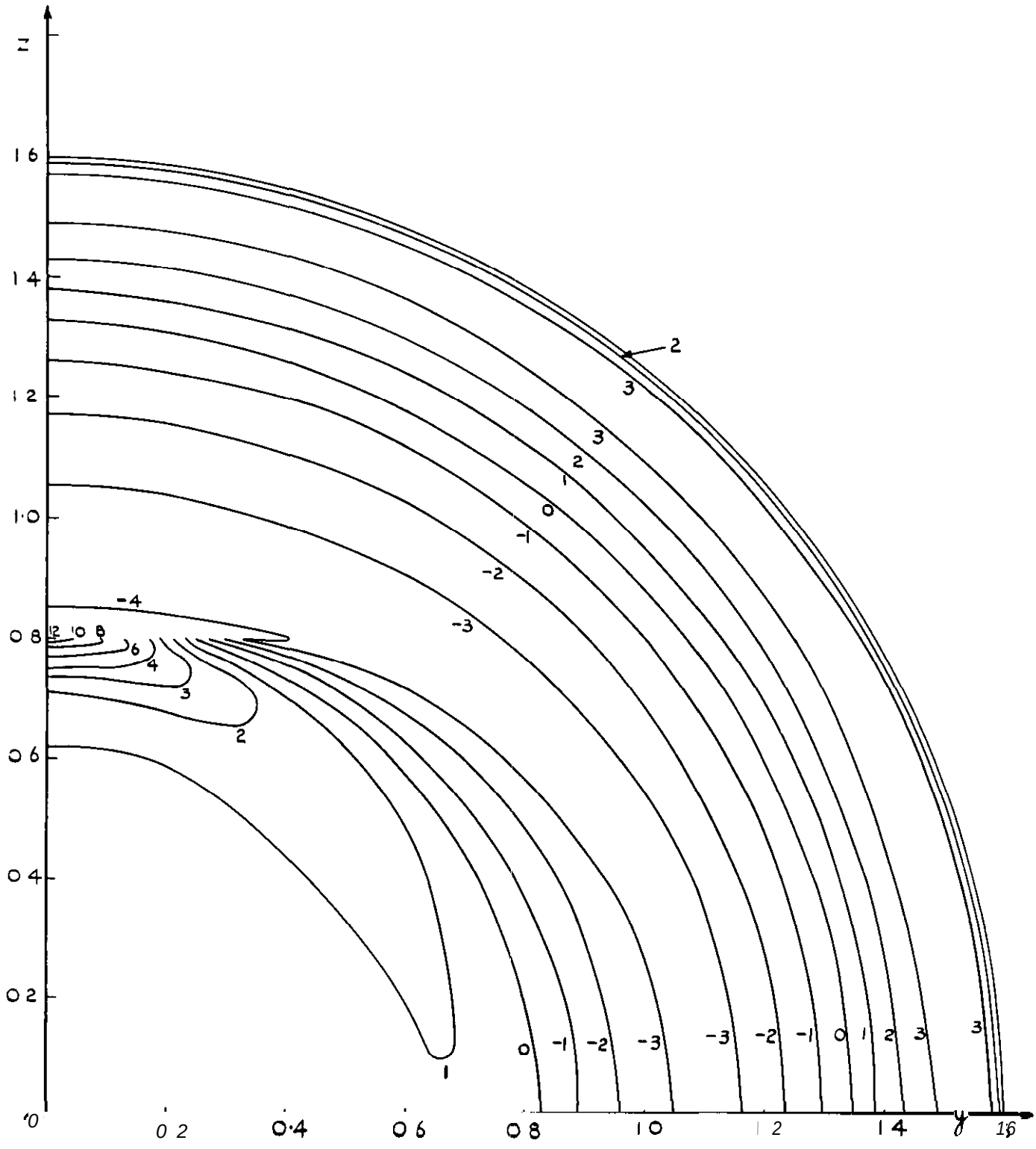

FIG. 8 ISOBARS IN THE PLANE X= 2;
$S=\frac{1}{3}$, M=1·6; β_S=0·41633

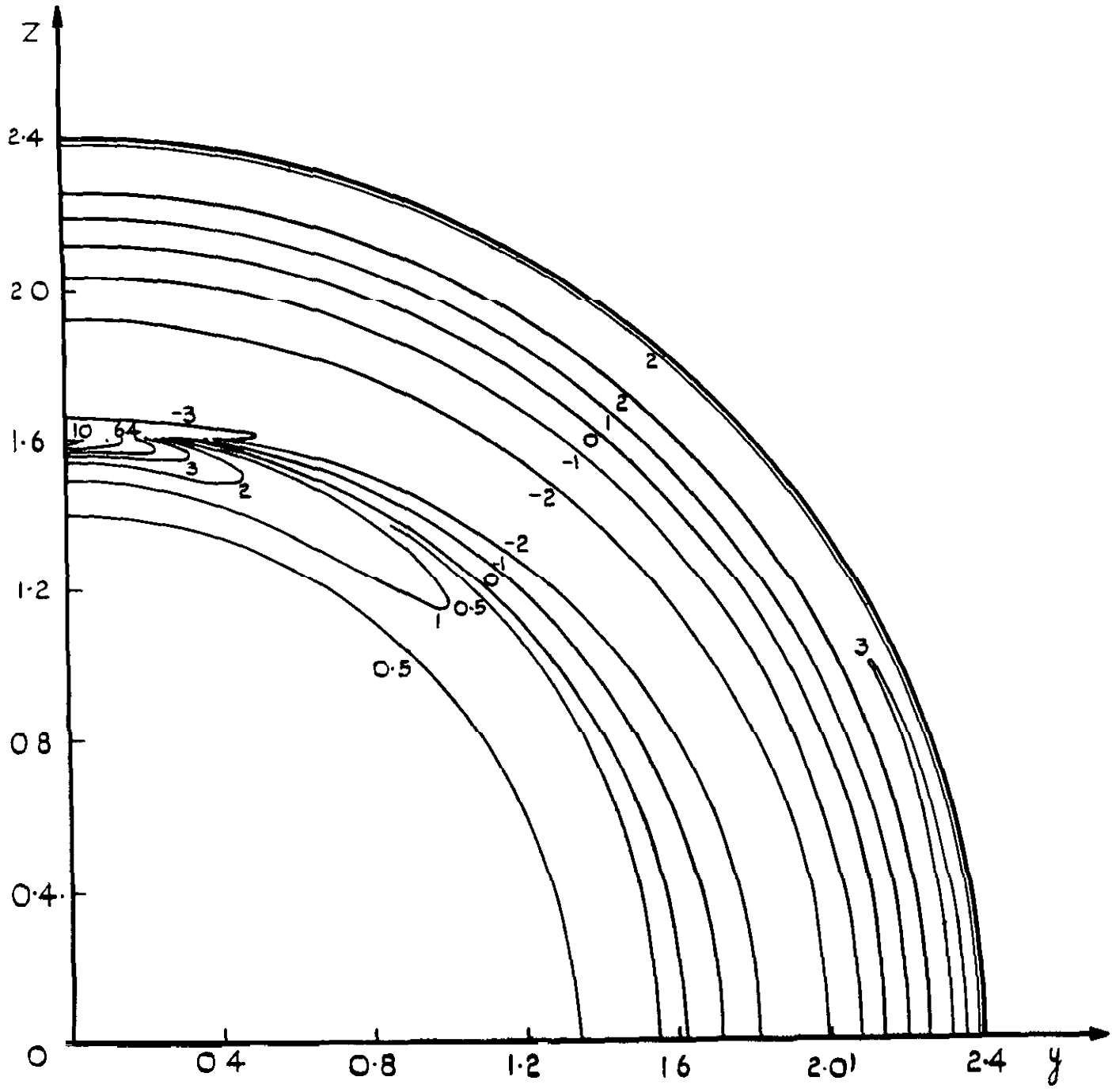

FIG. 9 ISOBARS IN THE PLANE X= 3 ;
$S=\frac{1}{3}$, $M=1\cdot6$; $\beta s=0\cdot41633$

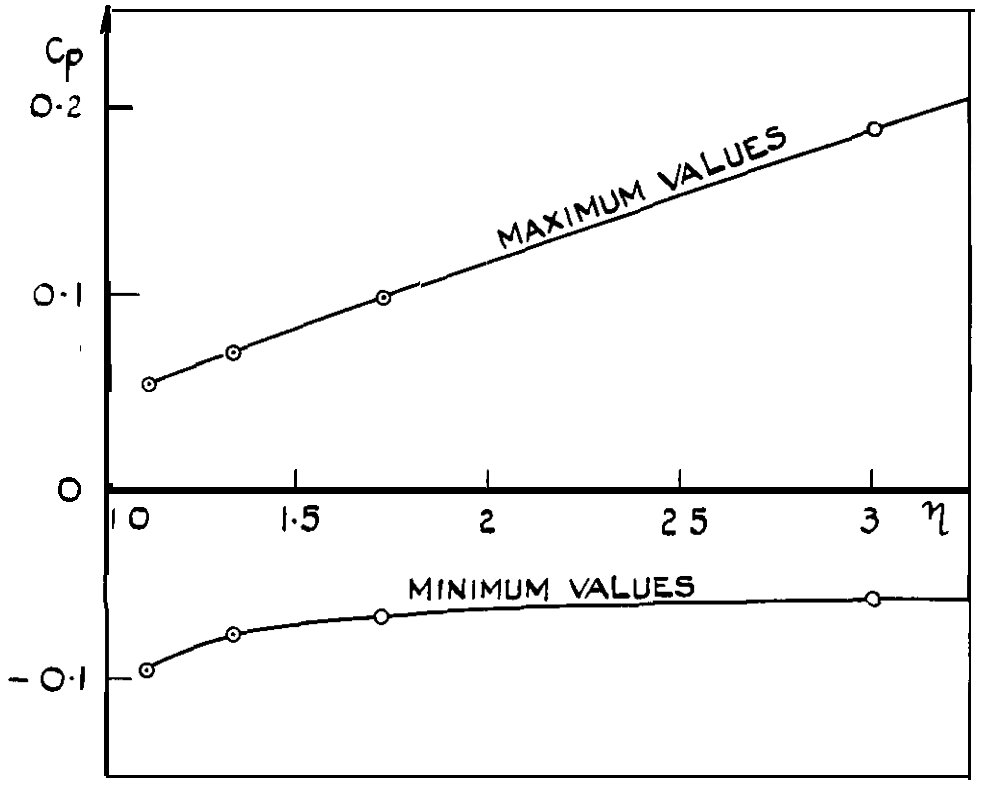

FIG 10 TURNING VALUES IN C_p ALONG THE LINE $X=0{\cdot}9999$, $Z=0$ AS FUNCTIONS OF η

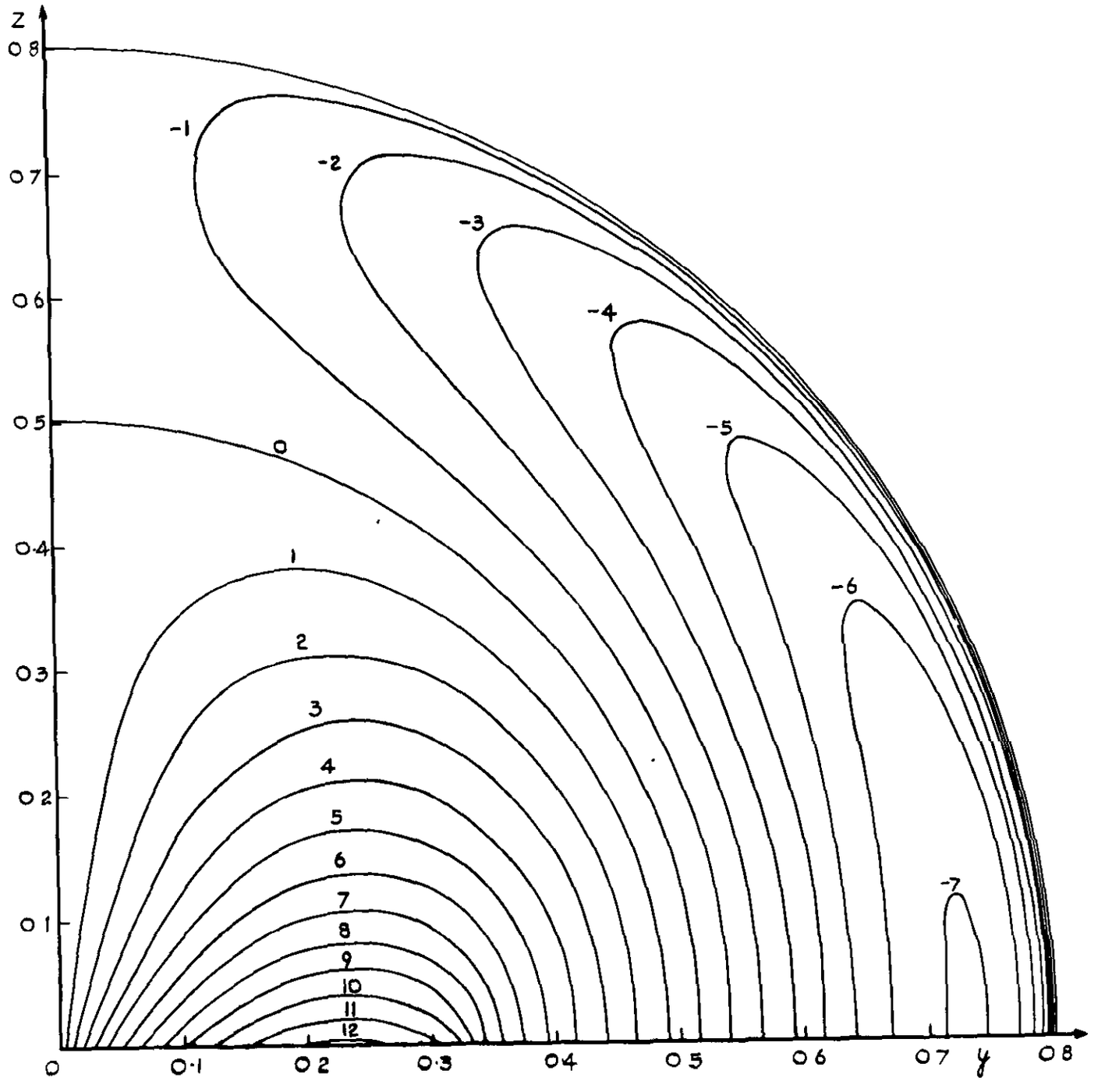

FIG.11 CURVES OF CONSTANT TRANSVERSE COMPONENT OF VELOCITY IN THE PLANE X=0·9999; S=$\frac{1}{3}$, M = 1·6; βS = 0-41633

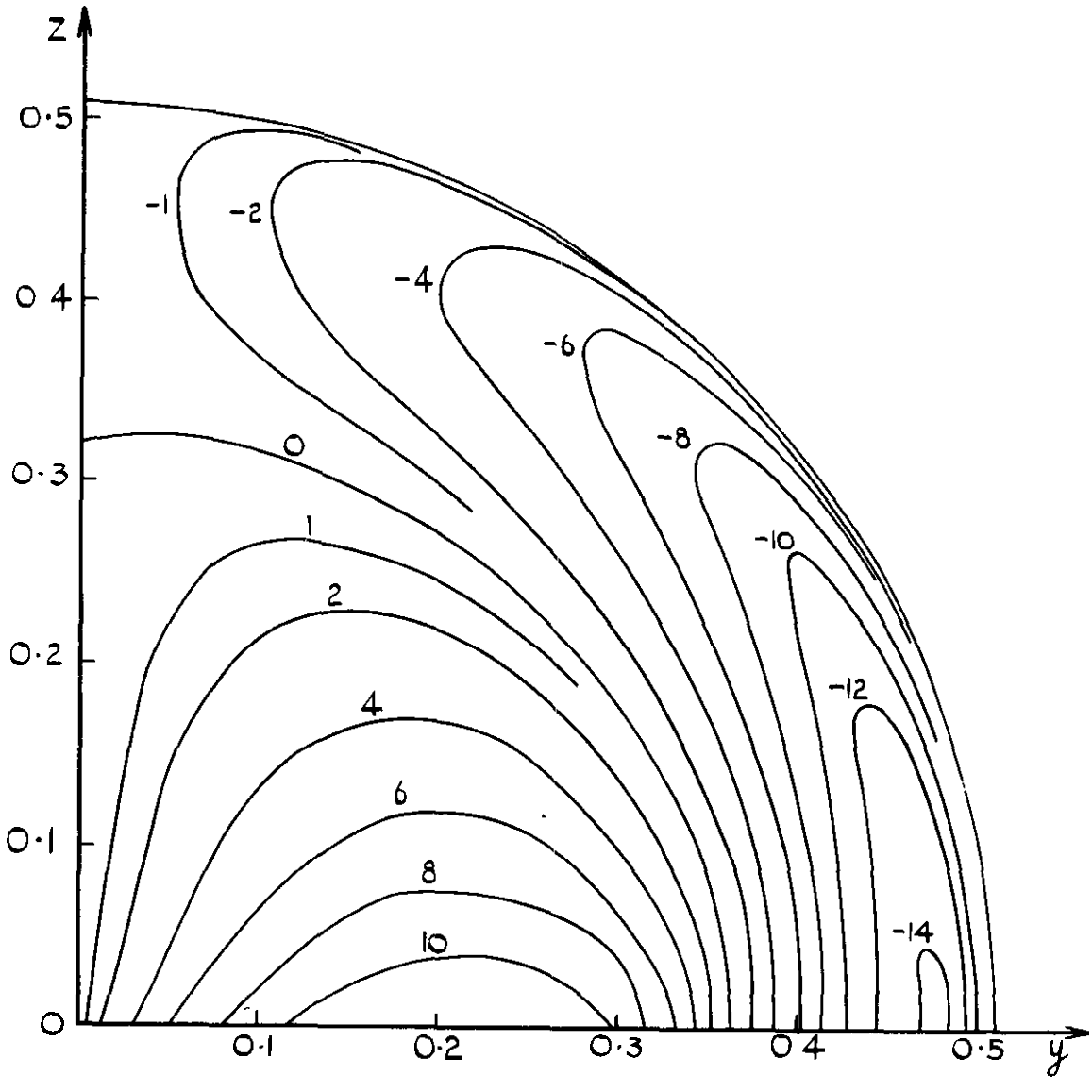

FIG.12 CURVES OF CONSTANT TRANSVERSE VELOCITY COMPONENT IN THE PLANE X= O-9999, $S=\frac{1}{3}$, M = 2 2; βs = O-65320

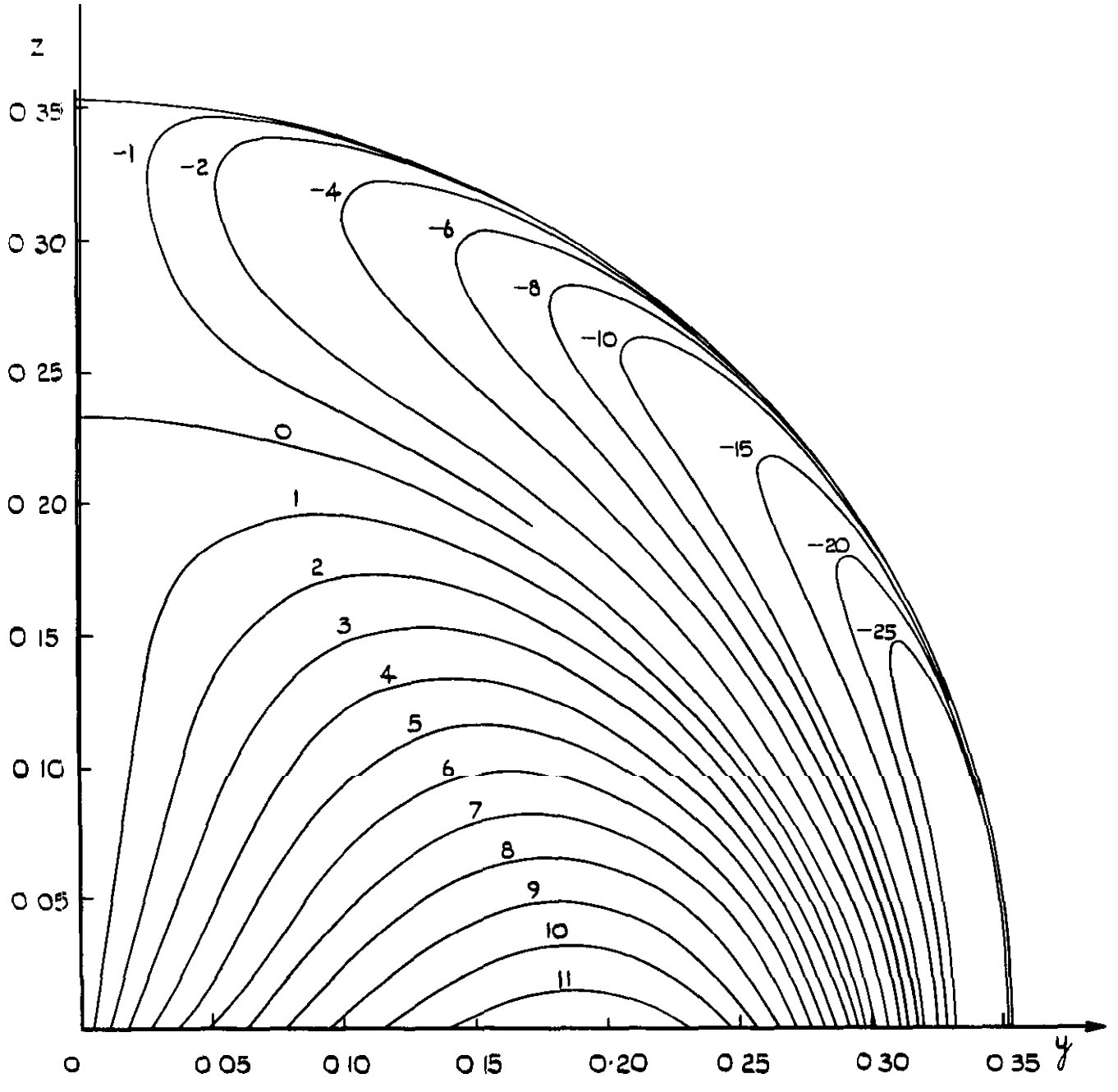

FIG.13 CURVES OF CONSTANT TRANSVERSE VELOCITY COMPONENT IN THE PLANE $X=0\cdot9999$; $S=\frac{1}{3}$, $M=3$; $\beta_S=0\cdot94281$

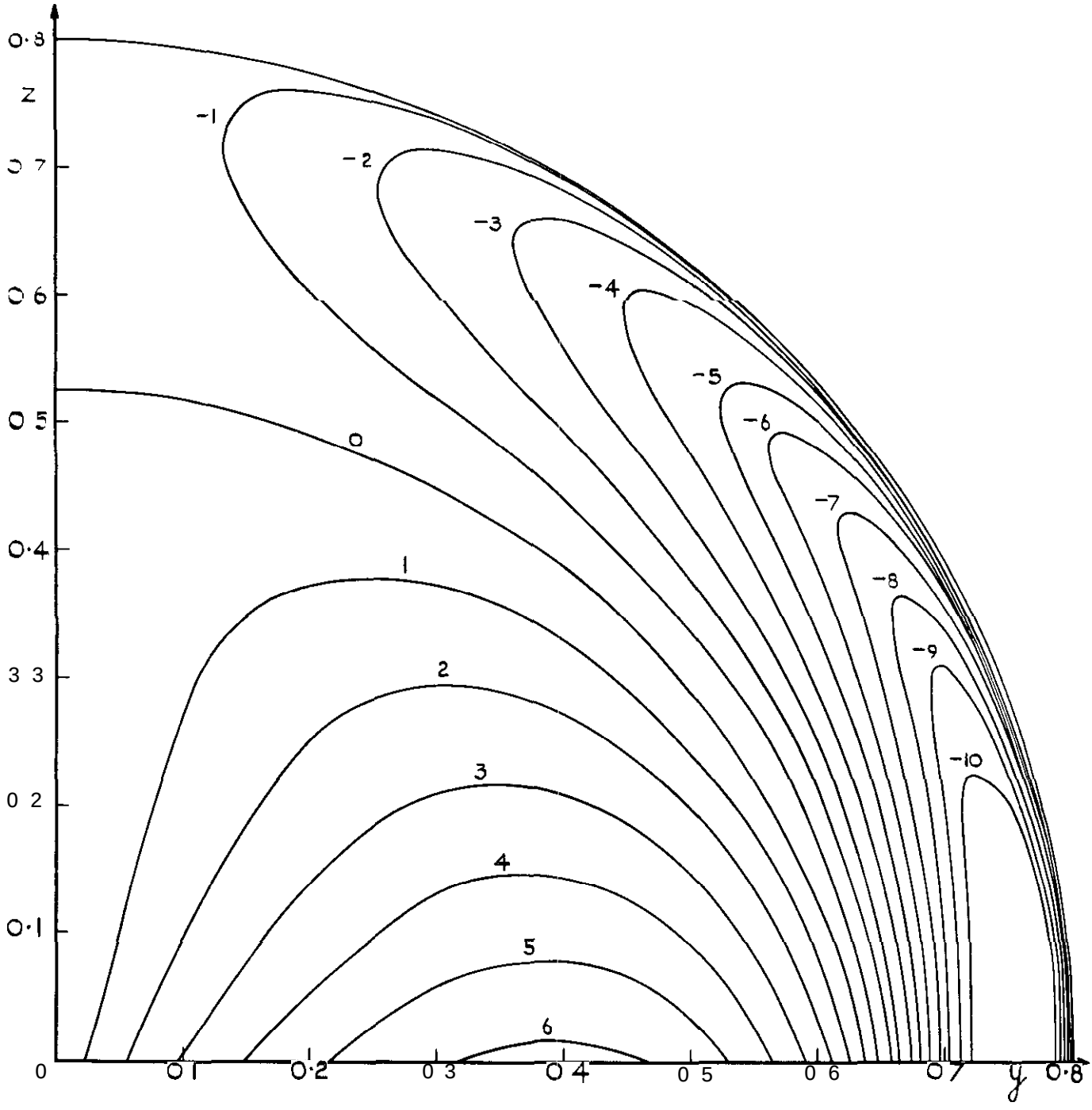

FIG. 14 CURVES Ok-CONSTANT TRANSVERSE VELOCITY COMPONENT IN THE PLANE X=O·9999; S=O·65, M=1·6; βs=O·81185

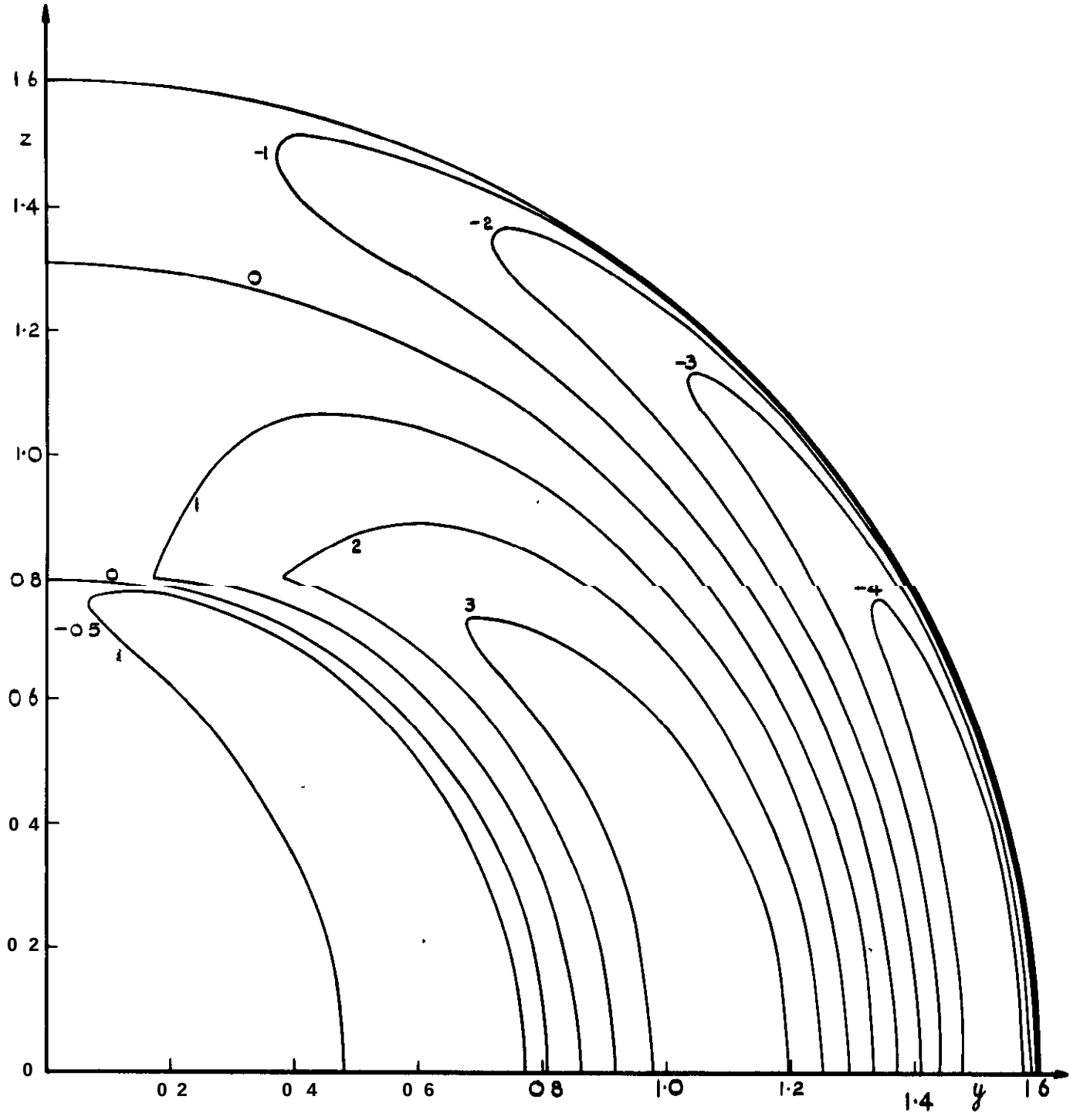

FIG. 15 CURVES OF CONSTANT TRANSVERSE VELOCITY COMPONENT IN THE PLANE X=2; S=$\frac{1}{3}$; M=1·6; β_S=0·41633

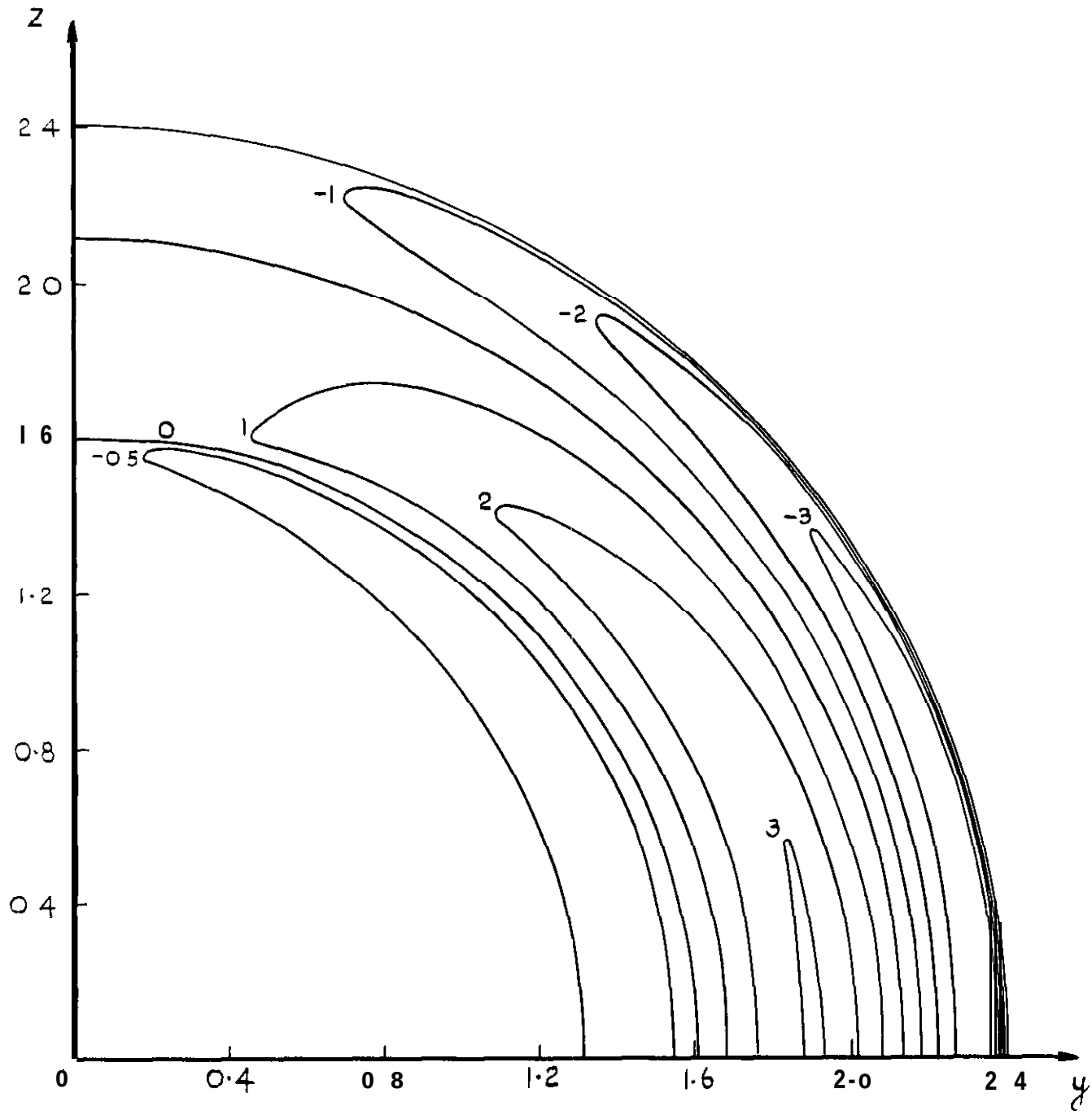

FIG 16 CURVES OF CONSTANT TRANSVERSE VELOCITY COMPONE N T IN THE PLANE X = 3 ; $S=\frac{1}{3}$, $M=1\cdot6$, $\beta s=0\cdot41633$

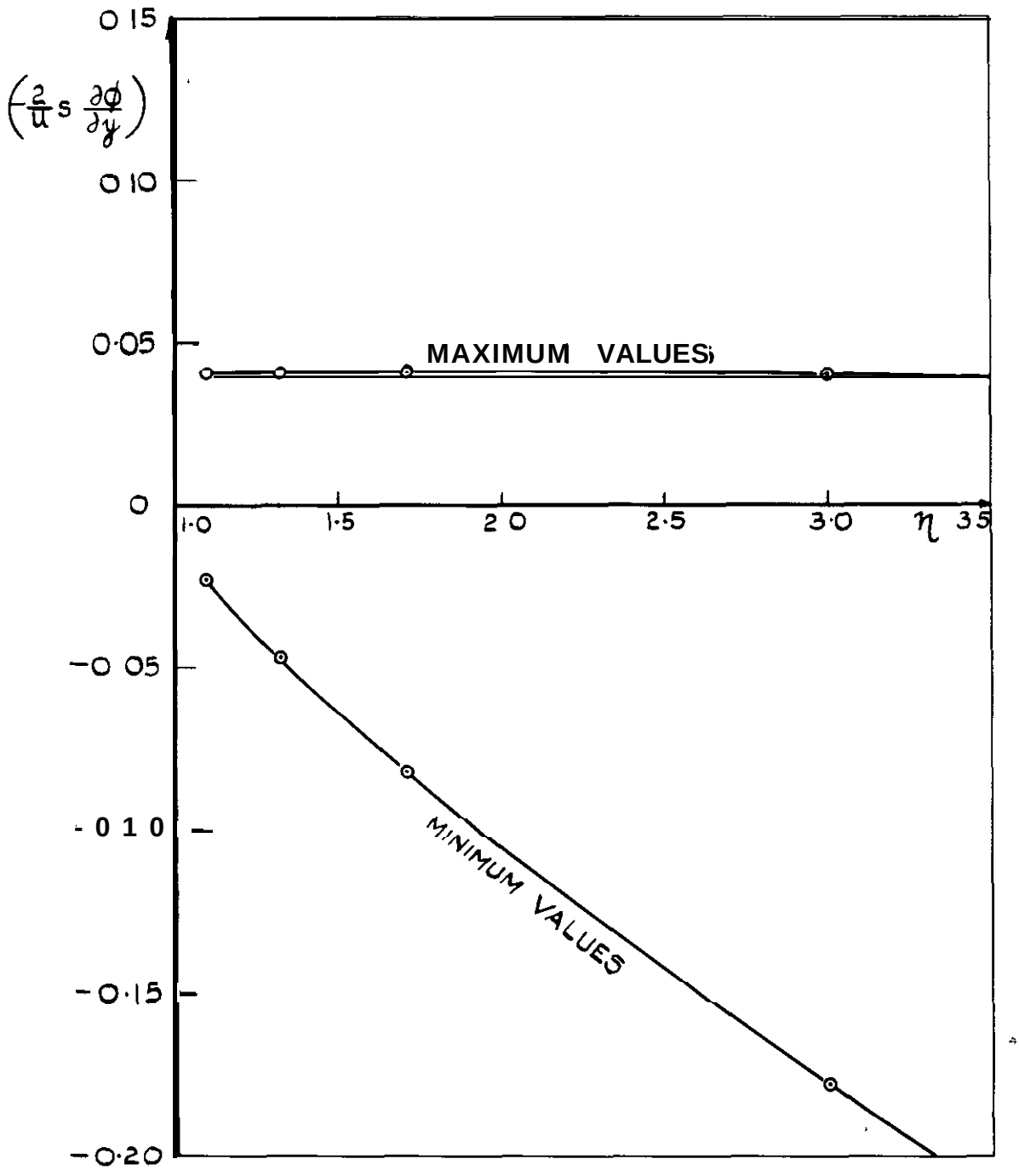

FIG.17 TURNING VALUES OF THE FUNCTION $\left(\frac{2}{u} s \frac{\partial \phi}{\partial y}\right)$ ALONG THE LINE X= 0.9999, Z=O,AS FUNCTIONS OF η

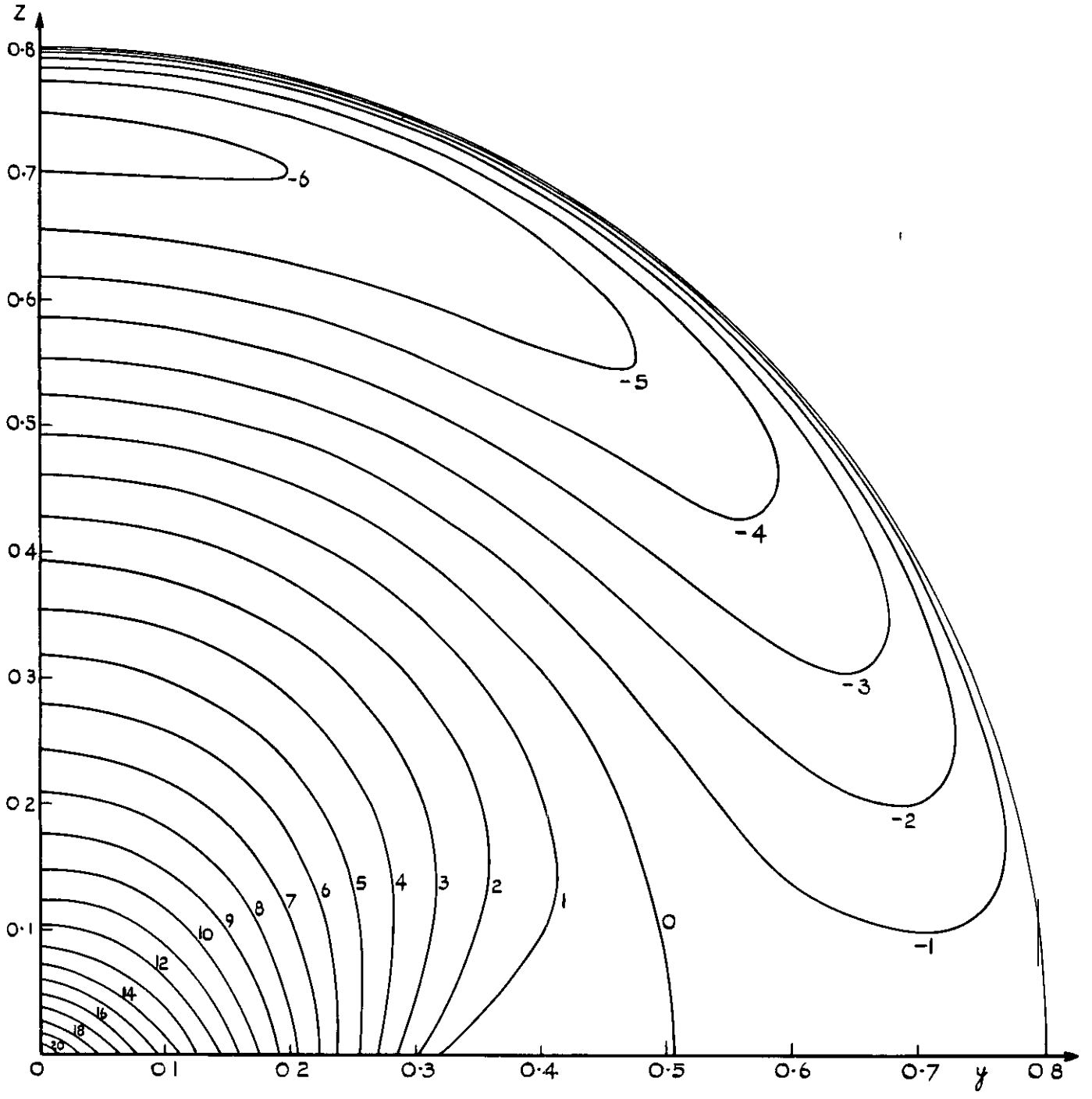

FIG.18 CURVES OF CONSTANT VERTICAL COMPONENT OF VELOCITY IN THE PLANE $X = 0{\cdot}9999$; $S = \frac{1}{3}$, $M = 1{\cdot}6$; $\beta S = 0{\cdot}41633$

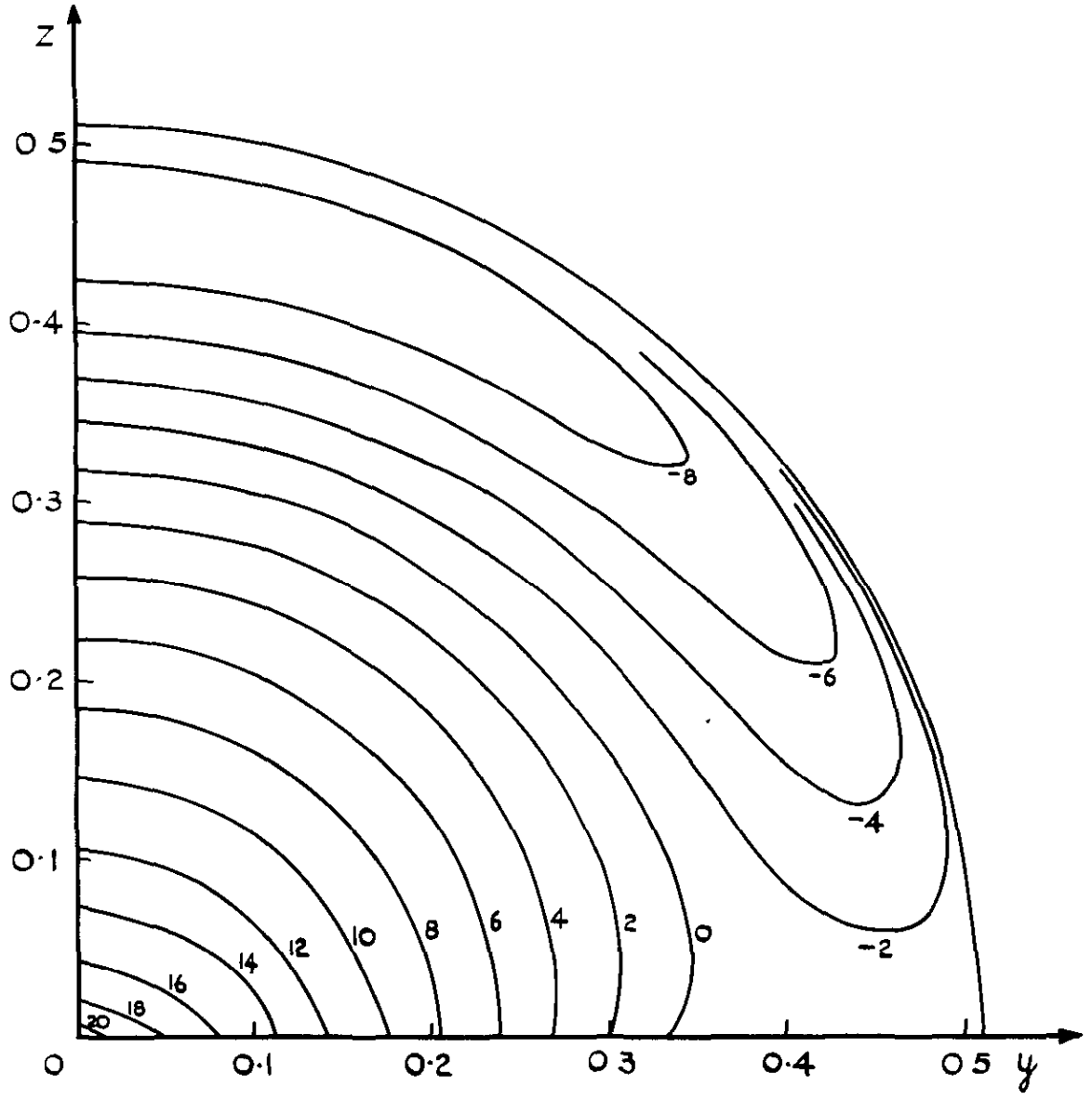

FIG. 19 CURVES OF CONSTANT VERTICAL VELOCITY COMPONENT IN THE PLANE X-O-9999, $S=\frac{1}{3}$, $M=2\cdot2$, $\beta s = 0.65320$

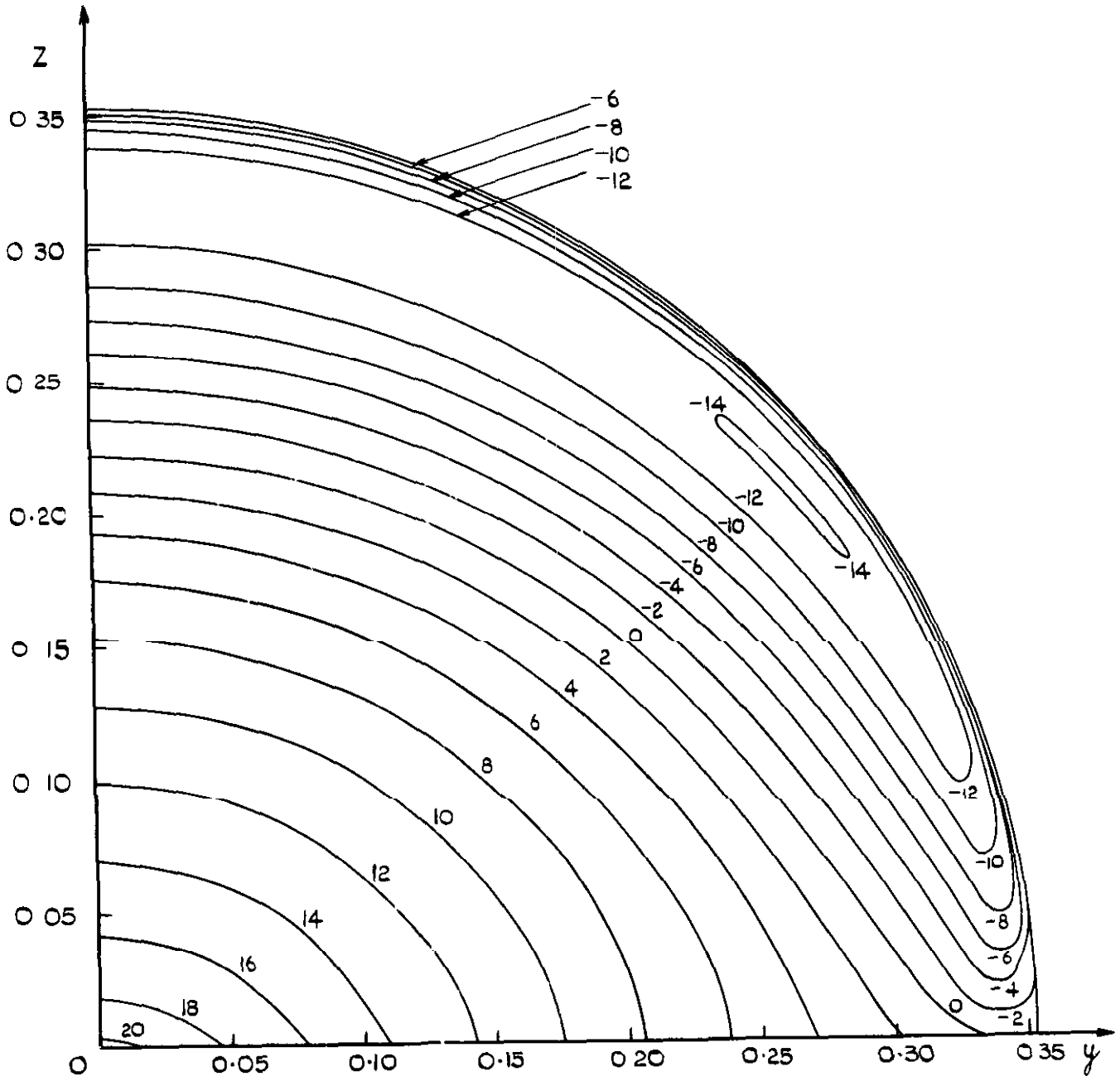

FIG. 20 CURVES OF CONSTANT VERTICAL VELOCITY COMPONENT IN THE PLANE X= 0·9999; S=$\frac{1}{3}$, M=3; βS = 0·94281

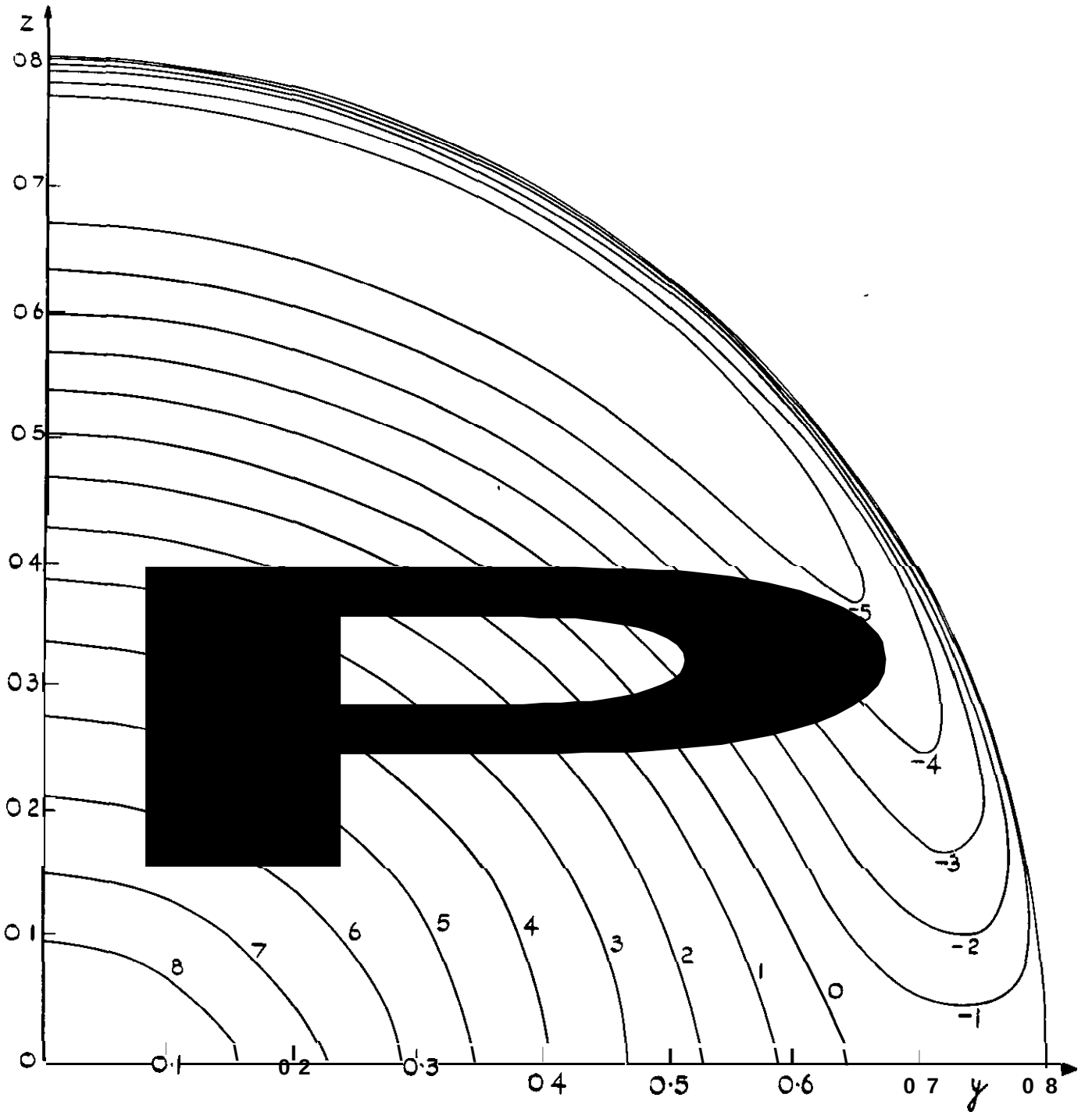

FIG.21 CURVES OF CONSTANT VERTICAL VELOCITY COMPONENT IN ME PLANE X=0·9999; S=0·65, M=1·6; β_S = 0-81185

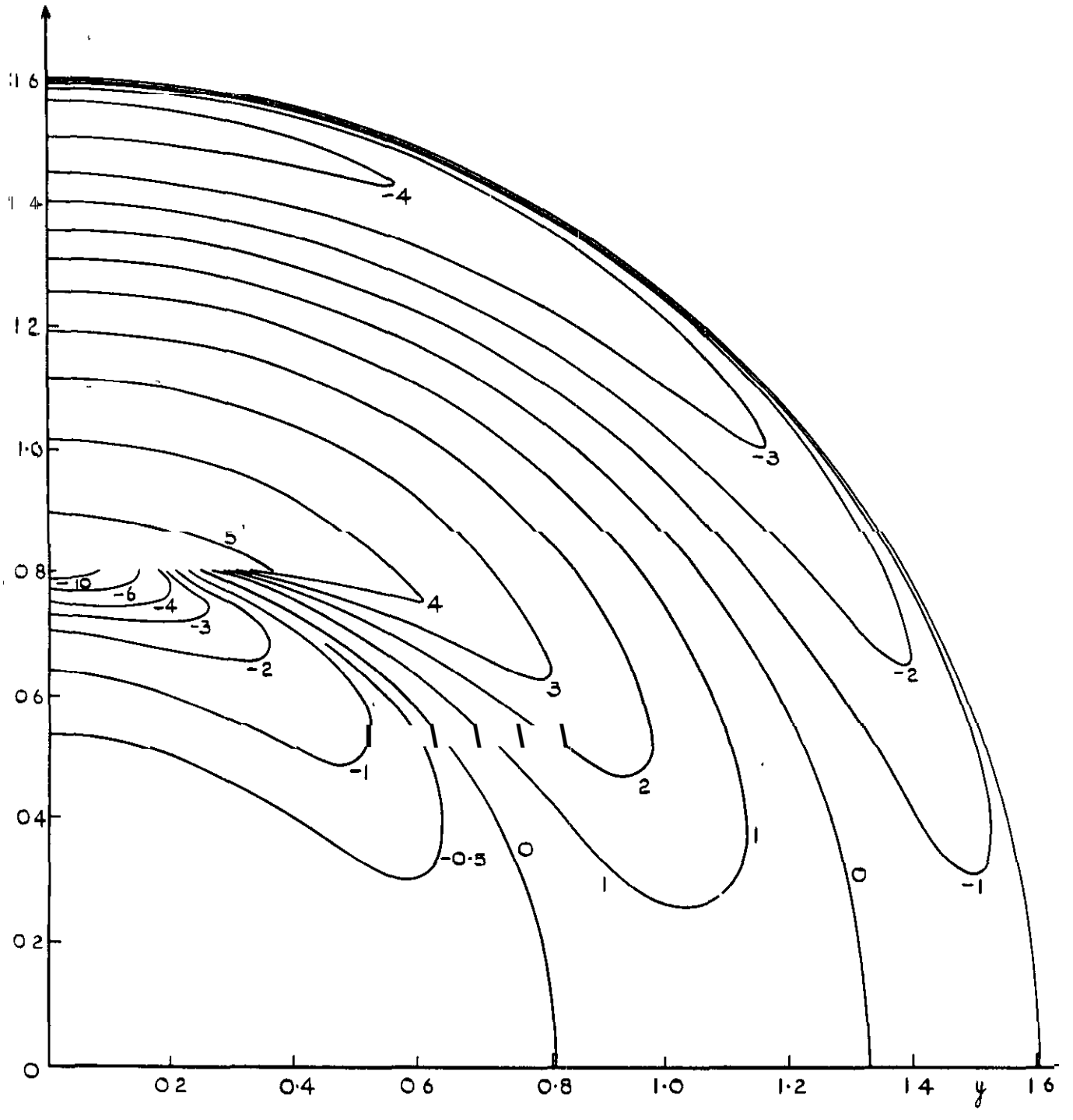

FIG.22; CURVES OF CONSTANT VERTICAL VELOCITY COMPONENT IN THE PLANE X= 2; S=$\frac{1}{3}$, M=1·6; βs=0·41633

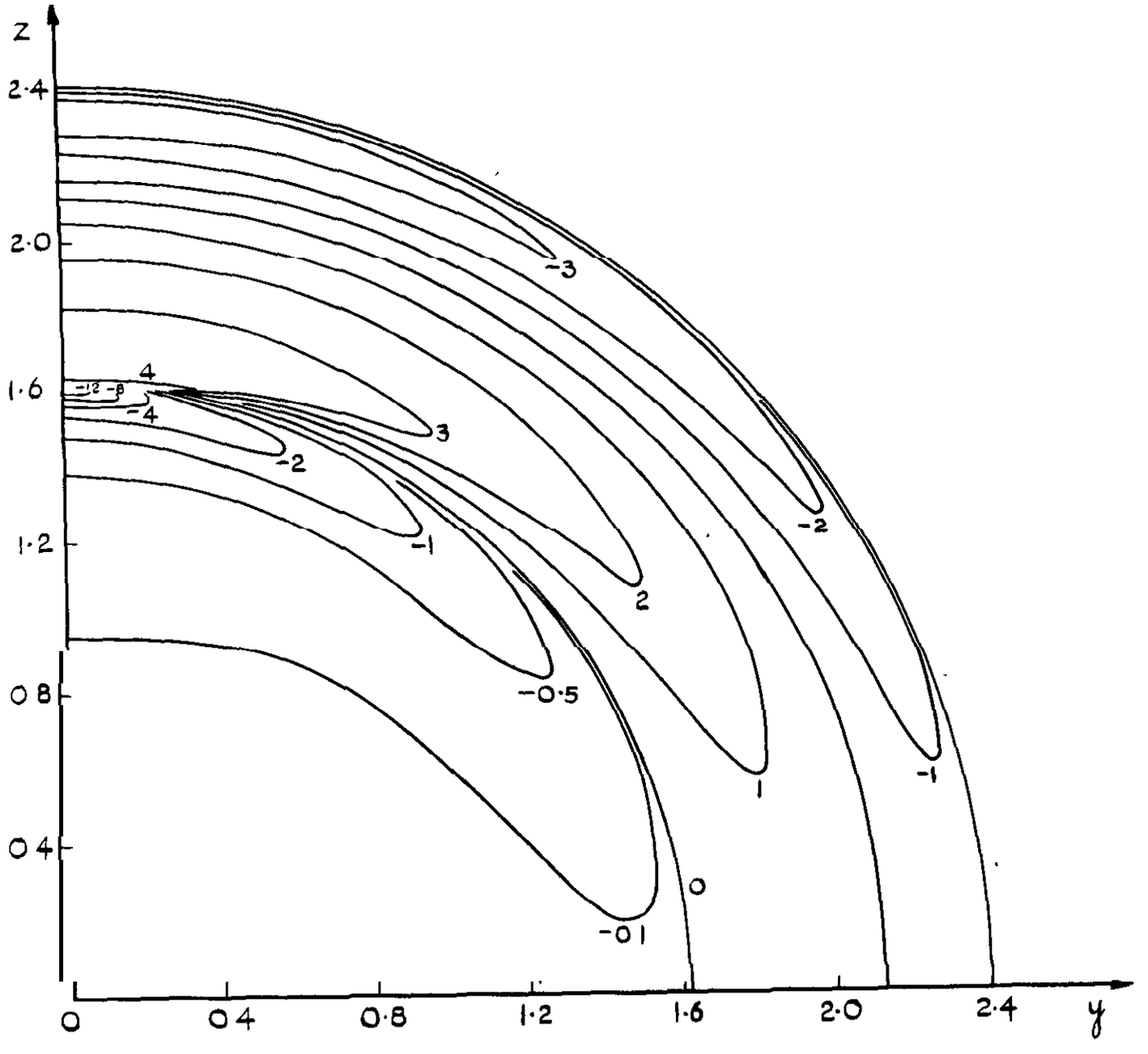

FIG 23 CURVES OF CONSTANT VERTICAL VELOCITY COMPONENT IN THE PLANE X=3; $S=\frac{1}{3}$, M=1·6; βs=0·41633

Printed in England for Her Majesty's Stationery Office by
the Royal *Aircraft Establishment, Farnborough.* Dd.129528. K.4.

ARC C.P. No.961
June 1966

Bartlett, R.S.

533.693.3 :
531.112 :
533.6.011.5 :
517.945

THE VELOCITY FIELD NEAR NON-LIFTING DELTA WINGS
ACCORDING TO SUPERSONIC LINEARIZED THEORY

The linearized theory of supersonic flow past thin wings Is used to obtain expressions for the three components of velocity of the flow about a family of non-lifting, symmetrical delta wings having rhombic cross-sections and subsonic leading edges. A Mercury Autocode programme has bee" written for their evaluation and results have bee" obtained for a particular wing for three Mach numbers and two values of the ratio of semi-spa" to centre-line chord. curve.5 of constant velocity, in planes normal to the free stream direction at and behind the trailing edge, are given for each velocity component.

ARC C.P. No.961
June 1966

Bartlett, R S .

533.693.3 :
531.112 :
533.6.011.5 :
517.945

THE VELOCITY FIELD NEAR NON-LIFTING DELTA WINGS
ACCORDING TO SUPERSONIC LINEARIZED THEORY

The linearized theory of supersonic flow past thin wings is used to obtain expressions for the three components of velocity of the flow about a family of non-lifting, symmetrical delta wings having rhombic cross-sections and subsonic leading edges. A Mercury Autocode programme has been written for their evaluation and results have bee" obtained for a particular wing for three Mach numbers and two values of the ratio of semi-span to centre-line chord. Curves of constant velocity, in planes normal to the free stream direction at and behind the trailing edge. are given for each velocity component.

ARC C.P. No.961
June 1966

Bartlett, R.S.

533.693.3 :
531.112 :
m.4011.5 :
517.945

THE VELOCITY FIELD NEAR NON-LIFTING DELTA WINGS
ACCORDING TO SUPERSONIC LINEARIZED THEORY

The linearized theory of supersonic flow past thin wings Is used to obtain expressions for the three components of velocity of th? flow about a family of non-lifting, symmetrical delta wings having rhombic cross-sections and subsonic leading edges. A Mercury Autocode programme has bee" written for their evaluation and results have bee" obtained for a particular wing for , three Mach numbers and two values of the ratio of semi-span to centre-line chord. Curves of constant velocity, in planes normal to the free stream direction at and behind the trailing edge, are given for each velocity component.

Published by
HER MAJESTY'S STATIONERY OFFICE

To be purchased from
49 High Holborn, London W.C.1
423 Oxford Street. London W 1
13A Castle Street, Edinburgh 2
109 St Mary Street, Cardiff
Brazennose Street, Manchester 2
50 Fairfax Street. Bristol 1
35 Smallbrook, Ringway, Birmingham 5
7-11 Linenhall Street, Belfast 2
or through any bookseller

C.P. No. 961

S.O. CODE No. 23-9017-61